2011

# Targeted knockdown of AMP-activated protein kinase alpha 1 and alpha 2 catalytic subunits

Larissa J. Tangeman
*Wright State University*

# TARGETED KNOCKDOWN OF AMP-ACTIVATED PROTEIN KINASE ALPHA 1 AND ALPHA 2 CATALYTIC SUBUNITS

A thesis submitted in partial fulfillment
of the requirements for the degree of
Master of Science

By

LARISSA JORDAN TANGEMAN
B.S., Wright State University, 2009

2011
Wright State University

WRIGHT STATE UNIVERSITY

GRADUATE SCHOOL

December 8, 2011

I HEREBY RECOMMEND THAT THE THESIS PREPARED UNDER MY SUPERVISION BY Larissa Jordan Tangeman ENTITLED TARGETED KNOCKDOWN OF AMP-ACTIVATED PROTEIN KINASE ALPHA 1 AND ALPHA 2 CATALYTIC SUBUNITS BE ACCEPTED IN PARTIAL FULFILLMENT OF THE REQUIREMENTS FOR THE DEGREE OF Master of Science

Thomas L. Brown, Ph.D.
Thesis Director

Barbara Hull, Ph.D.
Program Director

Committee on
Final Examination

Thomas L. Brown, Ph.D.

Christopher Wyatt, Ph.D.

Courtney Sulentic, Ph.D.

Andrew Hsu, Ph.D.
Dean, Graduate School

# ABSTRACT

Tangeman, Larissa Jordan. M.S., Microbiology and Immunology Program, Wright State University, 2011. Targeted Knockdown of AMP-activated Protein Kinase Alpha 1 and Alpha 2 Catalytic Subunits.

AMP-activated protein kinase (AMPK) regulates cellular metabolism and promotes ATP production when energy is depleted. Evidence suggests that AMPK may be involved in oxygen sensing by carotid body cells, which are responsible for regulating the breathing rate to maintain proper blood oxygen levels. There are two isoforms of the catalytic α subunit, AMPKα1 and AMPKα2, which could be involved in oxygen sensing. Here, the production of a short hairpin RNA (shRNA) targeting both catalytic isoforms of AMPK in human, mouse, and rat is described. The shRNA causes significant knockdown of both isoforms of AMPKα in mouse and human cells and a significant reduction in AMPK activity, measured as phosphorylation of a direct target. This shRNA will be used to generate a rat model with tissue-specific knockdown of AMPKα1 and 2 using a Cre-Lox recombination system to determine the role of AMPK in oxygen sensing by the carotid body.

TABLE OF CONTENTS

Page

I. INTRODUCTION . . . . . .1

AMP-activated protein kinase . . . . . .1

Carotid body . . . . . 2

Studying AMPK activity . . . . . .3

RNA interference . . . . . .3

Cre-Lox system . . . . . 7

Tissue-specific knockdown . . . . . .10

Summary . . . . . 13

II. MATERIALS AND METHODS . . . . . 16

Cloning and cell culture . . . . . .16

siRNA and shRNA design. . . . . 21

Transfection and infection . . . . . .22

Western blotting . . . . . 23

Data analysis . . . . . 24

III. RESULTS . . . . . 25

siRNA-mediated knockdown of AMPK alpha . . . . . 25

shRNA-mediated knockdown of AMPK alpha . . . . . .30

Knockdown of AMPK alpha in mouse and human cells . . . . . .35

Functional knockdown of AMPK alpha . . . . . 40

Expression of TH promoter-driven constructs. . . . . .40

Cre recombinase-driven recombination. . . . . 45

IV. DISCUSSION . . . . . 48

AMPK alpha 1 and 2 knockdown . . . . . 48

Tissue-specific constructs . . . . . 49

Disrupted U6 promoter . . . . . 50

Future work . . . . . 51

V. APPENDIX . . . . . .54

VI. REFERENCES . . . . . .55

LIST OF FIGURES

Page

Figure 1. Diagram of RNAi pathway . . . . . .5

Figure 2. Diagram of Cre recombinase-mediated recombination . . . . . 8

Figure 3. Structures of shRNA constructs . . . . . .11

Figure 4. Structure of virus producing tissue-specific silencing . . . . . 14

Figure 5. siRNA-mediated knockdown of AMPK alpha 1 and 2 in NIH3T3 cells . . . . .28

Figure 6. shRNA-mediated knockdown of AMPK alpha 1 and 2 in NIH3T3 cells with different loop sequences . . . . . .33

Figure 7. shRNA-mediated knockdown of AMPK alpha 1 and 2 in mouse and human cells . . . . . .36

Figure 8. Transfection efficiency of NIH3T3 and HEK293 cells . . . . . 38

Figure 9. shRNA-mediated knockdown of AMPK alpha activity in HEK293 cells . . . .41

Figure 10. Expression of TH promoter-driven constructs . . . . . .43

Figure 11. *In vitro* recombination of disrupted U6 promoter construct with Cre recombinase . . . . . 46

LIST OF TABLES

Page

Table 1. Base plasmids used to create constructs . . . . . 19

Table 2. Cloned constructs . . . . . .20

Table 3. Identification of a globally conserved sequence in AMPK alpha 1 and 2 . . . . .26

Table 4. Identification of a conserved sequence in AMPK alpha 2 . . . . . .27

Table 5. Design of shRNA loop sequences and sequences of shRNA oligos . . . . . .31

Table 6. Design of global AMPK alpha 1 and 2 shRNA and corresponding control shRNA . . . . . 32

# ACKNOWLEDGMENTS

I would like to acknowledge and thank the large number of people without whom this work would not have been possible. First, I would like to thank Dr. Thomas Brown for giving me the opportunity to work in his lab and for his continual assistance and support. This experience shaped my future career goals into what they are today. I would also like to thank my committee, Dr. Brown, Dr. Christopher Wyatt, and Dr. Courtney Sulentic, for their guidance throughout my project.

I would like to thank the members of the Brown Lab for their help and company for the past two years: Chanel Keoni, Renee Albers, Erica Baker, Rebecca Bricker, Deanne Jacobs, Christina Fung, Susan Robinson, Prakash Arumagum, Elizabeth Ludvigson, and Samantha Venkatesh. I would especially like to thank Renee and Erica for their excellent technical assistance and Chanel for helping me get my bearings when I first started. I would also like to thank the members of the Wyatt Lab, especially Dr. Wyatt, Barbara Barr, and Heidi Jordan, and Dr. R. Putnam for helping to create a very friendly and cooperative work environment.

I would like to thank Dr. James Lessard from Cincinnati Children's Hospital Medical Center for his gift of the anti-actin C4 antibody. I would like to thank Dr. C. Sulentic, Dr. C. Wyatt, Dr. T. Bubulya, Dr. M. Leffak, Dr. D. Cool, and Dr. J. Cambronero for allowing me to use their equipment, without which I could not have completed my project. I am very grateful to Dr. Michael Leffak for his cloning advice, which enabled me to complete a cloning step that had plagued me for almost a year.

I would like to thank the Microbiology and Immunology Program for providing me with financial support in the form of a teaching assistantship. This assistantship allowed me to afford graduate school, but it also gave me the opportunity to teach students and to recruit one of those students, Renee, to the Brown lab. I would also like to thank Dr. T. Bubulya and Meredith Rodgers for making my teaching experience enjoyable.

Finally, I would like to thank my family, especially my daughter Gabby, for their love and support, and Gabby would like to thank Dr. Brown for giving her Skittles every time she came to visit the lab.

# I. INTRODUCTION

*AMP-activated protein kinase*

Regulating energy levels is an essential process that occurs in all living organisms. AMPK (5'-adenosine monophosphate-activated protein kinase), also known as protein kinase, AMP-activated (PRKAA), is an enzyme that is conserved from yeast to humans and has important roles in sensing the energy status of the cell to maintain homeostasis [1-5]. AMPK has been linked to numerous disease states, including metabolic disorders and cancer, although its role is still not clear and appears to be context-dependent [6]. Functional AMPK is a heterotrimer that acts to regulate metabolism and is composed of three subunits, the catalytic alpha subunit and the regulatory beta and gamma subunits [3,7]. There are two isoforms of the AMPK alpha subunit, AMPK$\alpha$1 and AMPK$\alpha$2, and each isoform has been shown to have overlapping as well as distinct functions depending on the cell type [3,8-11].

AMPK acts as a metabolic master switch regulating several intracellular systems including glucose uptake and β-oxidation of fatty acids. AMPK inhibits fatty acid synthesis by phosphorylating acetyl-CoA carboxylase (ACC) at Ser79 [12]. The energy-sensing capability of AMPK can be attributed to its ability to detect and react to

fluctuations in the AMP: ATP ratio. Stressors, such as muscle contraction or ischemia, that deplete ATP in the cell result in an elevated AMP: ATP ratio, triggering AMPK activation. AMPK is phosphorylated at Thr172 of the alpha subunit by LKB1, a known tumor suppressor [13], and calmodulin-dependent protein kinase kinase β (CaMKKβ) [14], and this phosphorylation is required for activation. AMP activates AMPK by inhibiting the dephosphorylation of Thr172 by protein phosphatase-2C [5,8]. AMPK is also allosterically activated by AMP binding to the γ subunit [8]. Activated AMPK promotes ATP production and inhibits anabolic pathways that utilize ATP.

*Carotid body*

In addition to its other roles, AMPK may be involved in oxygen sensing. The carotid body is a small paired sensory organ which is responsible for sensing oxygen levels in the carotid artery and signaling through the carotid sinus nerve to regulate the breathing rate in order to maintain oxygen homeostasis [15]. The carotid body is composed of two types of cells; type I cells sense oxygen through an unknown mechanism, and type II cells appear to provide support [16]. AMPK has been reported to couple hypoxic inhibition of mitochondrial oxidative phosphorylation to excitation of isolated rat carotid body type I cells [17]. To determine if AMPK is necessary for oxygen sensing by carotid body type I cells, we decided to generate an AMPK-deficient rat model to study the ability of the animals to respond to hypoxia. Rats were chosen because the carotid body has been studied extensively in the rat [16]. It is not known which isoform of AMPKα may be involved in oxygen sensing or if they can both perform the same function in the carotid body. For this reason, we wanted to inhibit both

isoforms. These rats will be used to determine if AMPK is required *in vivo* for the carotid body to upregulate the breathing rate in response to hypoxia.

*Studying AMPK activity*

Multiple strategies to manipulate AMPK activity have been developed. Drugs targeting AMPK, such as the activating drug AICAR (5-aminoimidazole-4-carboxyamide ribonucleoside) and inhibitor Compound C, have been identified, but these pharmacological agents have been shown to alter other processes in the cell as well [18-19]. For example, AICAR is metabolized in the cell into an AMP analogue that is able to bind AMP-binding sites on other proteins and is also able to inhibit oxidative phosphorylation independent of its effect on AMPK [18]. Compound C has been shown to inhibit over 10 kinases, not just AMPK [19]. Therefore, these drugs do not specifically target AMPK, and alternate methods should be used to alter AMPK activity more precisely. The generation of AMPKα1 (α1-/-) and α2 (α2-/-) knockout mice have established critical roles for AMPKα1 and AMPKα2 in the regulation of energy metabolism and oxygen sensing [3,9,20]. Double knockout of the AMPKα1 and AMPKα2 isoforms, simultaneously, results in lethality at embryonic day 10.5 [3], so this model system is not available to study functions that can be performed by both isoforms of AMPKα. An alternative method to inhibit AMPKα1 and 2 is needed.

*RNA interference*

Another way to study the activity of AMPK is to block its expression using RNA interference. RNA interference (RNAi) is a process by which double-stranded RNA

(dsRNA) molecules can regulate gene expression. Small interfering RNAs (siRNAs), are synthetic, 21-nucleotide dsRNA molecules that are complementary to a mRNA transcript [21]. As shown in Figure 1, when siRNA is introduced into a cell, one strand is incorporated into the RNA-induced silencing complex (RISC) and binds the complementary mRNA [22]. This results in destruction of the mRNA transcript by a member of the Argonaute family of proteins [23], thus preventing translation into protein [24-25]. The effects of siRNA are transient because the siRNA molecules get diluted as the cells divide [26]. Therefore, this strategy is not useful for long-term studies.

Short hairpin RNAs (shRNAs) are synthetic RNA molecules that have been modified to include a stem-loop-stem structure resembling the structure of naturally-occurring microRNAs (miRNAs). As shown in Figure 1, the hairpin structure of shRNAs is cleaved by the enzyme Dicer in the cytoplasm into siRNA molecules [27]. shRNAs are transcribed from DNA templates such as plasmids, and this allows their expression to be stable and heritable in cell culture [28-31]. The RNA polymerase III promoters U6 and H1, which are the promoters for the U6 small nuclear RNA and histone H1 respectively, are commonly used to drive expression of shRNAs [32]. In addition, shRNAs can be used to generate transgenic animal models with knockdown of target proteins as an alternative to classic transgenic animal knockout models. A number of silencing RNAs against AMPK have been generated [2,10,33-34], but there is no

**Figure 1. Diagram of RNAi pathway**

Diagram of the siRNA and shRNA pathways after transcription of an shRNA from a DNA template in the nucleus or introduction of synthetic siRNA molecules directly into the cytoplasm of the cell. Arrows indicate molecules that must be introduced into the cell through transfection or another method to generate knockdown: DNA template such as a plasmid or virus (shRNA) or dsRNA molecules (siRNA).

**Figure 1**

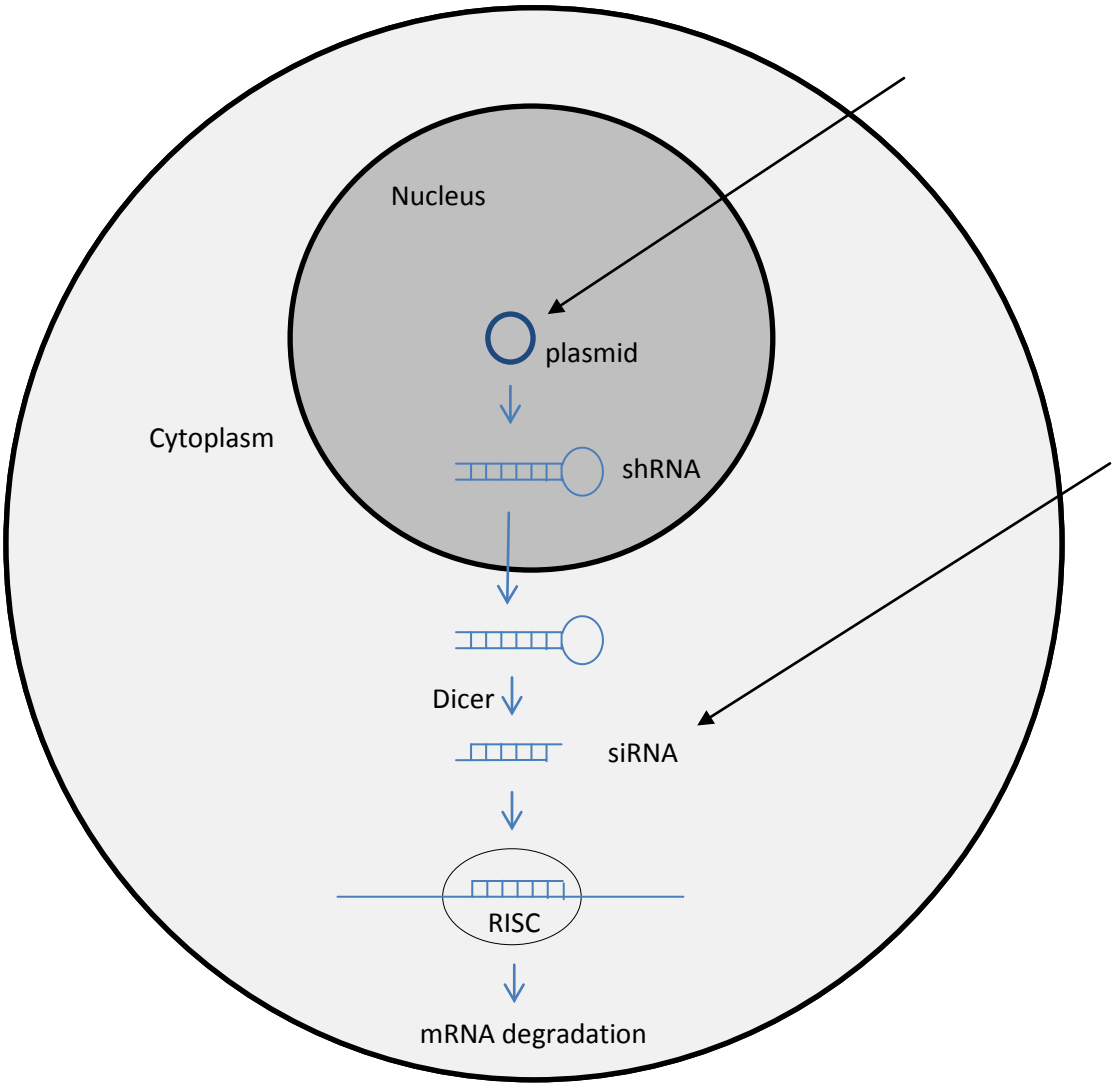
Nucleus
plasmid
Cytoplasm
shRNA
Dicer
siRNA
RISC
mRNA degradation

reported sequence that is able to knock down both catalytic isoforms of AMPKα1 and AMPKα2 in multiple species. For this reason, we designed an shRNA that is complementary to a sequence conserved between both catalytic isoforms in human, mouse, and rat and can be used in any of these three model systems.

*Cre-Lox system*

We will use Cre recombinase to direct the tissue-specific expression of an shRNA against AMPKα1 and 2. Cre recombinase is an enzyme that catalyzes site-specific DNA recombination at sequences called LoxP sites [35]. LoxP sites are 34-basepair stretches of DNA containing two 13-basepair palindromes separated by an 8-basepair spacer, which confers directionality to the site; the region of DNA flanked by two LoxP sites is said to be "floxed" [36]. The Cre enzyme binds to LoxP sites in the DNA and aligns two sites in the same orientation. It then catalyzes a recombination reaction in which the floxed DNA sequence and one of the two LoxP sites are excised from the DNA (Figure 2). This technique is used to delete genes or other stretches of DNA. Cre recombinase has been used to create animal models with tissue-specific knockout of genes by mating mice with floxed genes to mice with tissue-specific expression of the Cre recombinase enzyme [originally described in 37]. The offspring resulting from the mating have knockout of the floxed gene only in tissues where Cre recombinase is expressed. This powerful technique has been used numerous times to create animal models, especially when the total body knockout causes embryonic lethality.

**Figure 2. Diagram of Cre recombinase-mediated recombination**

DNA recombination catalyzed by Cre recombinase at LoxP sites located between DNA regions A and B and regions B and C. Region B is the floxed DNA that is removed following binding of Cre recombinase at LoxP sites, looping of the DNA, aligning of the LoxP sites, and recombination.

**Figure 2**

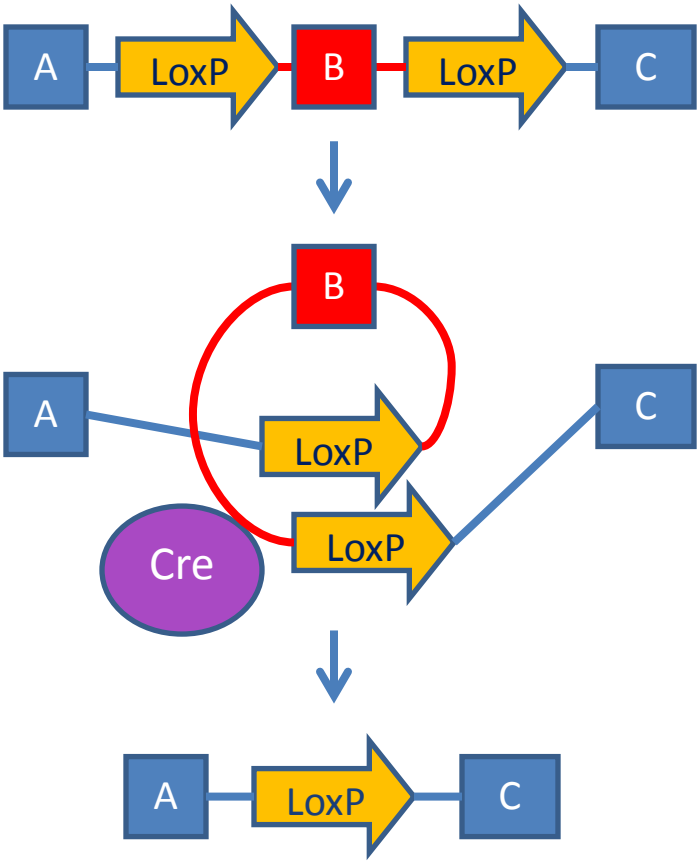

*Tissue-specific knockdown*

Tissue-specific knockdown will be accomplished by disrupting the U6 promoter, which controls the expression of the shRNA, with a floxed sequence of DNA containing an RNA polymerase III stop sequence. The promoter will not be active, and the shRNA will not be transcribed, unless the extra DNA is removed. Figure 3 shows a diagram of a standard shRNA under control of the U6 promoter, an shRNA with a disrupted U6 promoter, and a schematic of the recombination that would occur following the expression of Cre recombinase. Tissue-specific expression of Cre recombinase will allow the promoter to be restored, and the shRNA will only be made in tissues that express Cre recombinase.

The tissue-specific promoter that was chosen to direct the expression of Cre recombinase is the tyrosine hydroxylase (TH) promoter. Tyrosine hydroxylase is an enzyme that catalyzes the conversion of L-tyrosine to DOPA, the rate-limiting step of catecholamine synthesis [38], and it is only expressed in carotid body type I cells [39] and in the brain and adrenal glands [40]. The shRNA will only be made in cells that express tyrosine hydroxylase. The TH promoter was chosen because TH is known to be highly expressed in carotid body type I cells, and TH is frequently used as a marker for type I cells [39]. It is possible that there could be off-target effects on breathing regulation due to knockdown of AMPK$\alpha$ in other tissues.

Both of the components necessary to generate tissue-specific knockdown of AMPK$\alpha$1 and 2 will be cloned into one construct that can be used to make a lentivirus.

**Figure 3. Structures of shRNA constructs**

(A) Structure of the shRNA under control of the U6 promoter. (B) Structure of the shRNA with disrupted U6 promoter. (C) Diagram of recombination that would occur following expression of Cre recombinase with the construct shown in B.

**Figure 3**

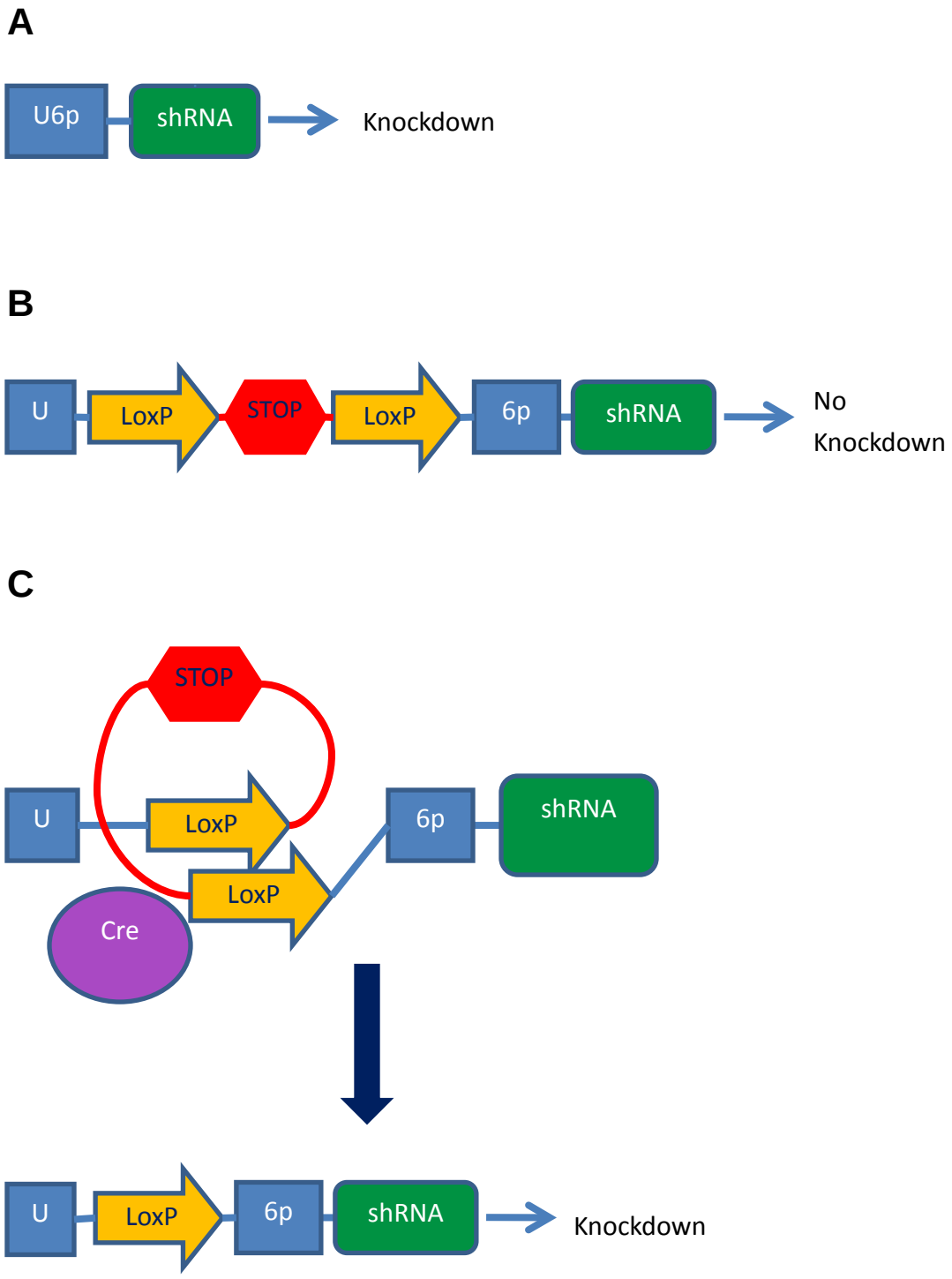
A
U6p
shRNA
Knockdown
B
U
LoxP
STOP
LoxP
6p
shRNA
No
Knockdown
C
STOP
U
LoxP
6p
shRNA
LoxP
Cre
U
LoxP
6p
shRNA
Knockdown

Figure 4 shows a diagram of this final construct. The virus will contain both the shRNA with a disrupted U6 promoter and the Cre recombinase gene under control of the TH promoter. Also shown in Figure 4 is a diagram of the recombination that would occur in tissues that activate the TH promoter and, therefore, express Cre recombinase. This construct will be made into a lentivirus because the virus can be used to infect embryos in order to generate a transgenic rat strain with tissue-specific knockdown of AMPKα1 and 2.

*Summary*

In this study, we demonstrate the production of a novel shRNA that simultaneously targets both AMPKα1 and α2 isoforms. This shRNA is 100% complementary to a nucleotide sequence conserved in the human, mouse, and rat forms of the AMPKα1 and AMPKα2 mRNA and causes a significant reduction in AMPKα1 and 2 protein levels. Knockdown of AMPKα1 and 2 also reduces phosphorylation of ACC, a direct target of AMPK. This new shRNA will be useful for analyzing the numerous functional roles of AMPKα1 and 2, and it will later be used to generate a transgenic rat strain with tissue-specific silencing of AMPKα1 and 2. These rats will be studied to determine if AMPK is involved in the oxygen-sensing capabilities of carotid body type I cells.

**Figure 4. Structure of virus producing tissue-specific silencing**

(A) Structure of the virus. (B) Diagram of recombination that would occur in tissues that activate the TH promoter and express Cre recombinase.

**Figure 4**

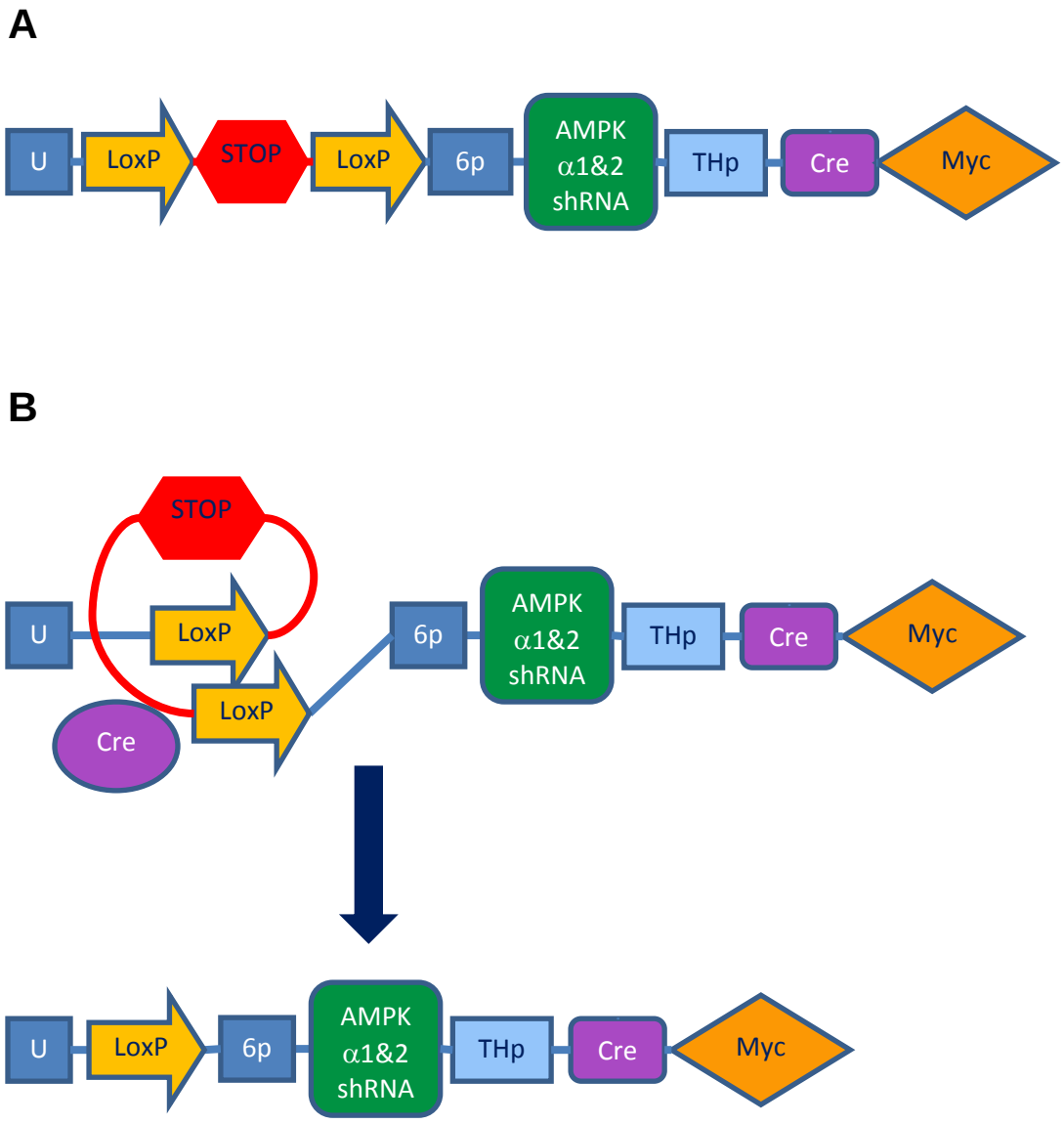
A
U
LoxP
STOP
LoxP
6p
AMPK
α1&2
shRNA
THp
Cre
Myc
B
STOP
U
LoxP
LoxP
Cre
6p
AMPK
α1&2
shRNA
THp
Cre
Myc
U
LoxP
6p
AMPK
α1&2
shRNA
THp
Cre
Myc

# II. MATERIALS AND METHODS

*Cloning and cell culture*

Restriction enzymes and buffers used in ligation experiments were purchased from Invitrogen (Carlsbad, CA) and used according to the manufacturer's specifications. Digested vector DNA was dephosphorylated using Antarctic Phosphatase (New England Biolabs, Ipswich, MA, M0289S) prior to ligation. Digested DNA was separated using agarose gel electrophoresis, and DNA fragments for ligation were isolated using an E.Z.N.A. Gel Extraction Kit (Omega Bio-Tek, Norcross, GA, D2501-01) according to the manufacturer's specifications. All ligations were performed using a rapid ligation kit (Roche, Basel, Switzerland, 11635379001) according to the manufacturer's specifications. Lentiviral plasmids were transformed into One Shot Stbl3 Chemically Competent Cells (Invitrogen, Carlsbad, CA, C7373-03) according to the manufacturer's specifications. Plasmid DNA was isolated from bacterial cultures using E.Z. Nucleic Acid Plasmid Mini (D6942-02) or Maxi (D6922-02) Kits from Omega Bio-Tek (Norcross, GA) according to the manufacturer's specifications. Sequences were verified by DNA sequencing (AGCT, Inc., Wheeling, IL). Table 1 contains a summary of base plasmids used as starting materials for cloning. Table 2 contains a summary of all cloned plasmid constructs.

A multiple cloning site, or MCS, (ClaI-XbaI-NdeI-HindIII-EcoRV-EcoRI-PstI-SmaI-SalI-XbaI-BamHI) was purchased as DNA oligonucleotides from IDT, Inc. (Coralville, IA), annealed, and ligated into pLenti6/V5 D-TOPO™ (Invitrogen, Carlsbad, CA, K4955-01) containing an enhanced green fluorescent protein (GFP) gene using ClaI and BamHI to create pLv-MCS-GFP.

The rat tyrosine hydroxylase promoter was isolated from 4.5ThpAL+ (provided by Dr. Karen O'Malley, Washington University School of Medicine) using EcoRV and EcoRI and cloned into the MCS to create pLv-MCS-THp-GFP. This construct was used to generate a stable pool of HEK293 cells expressing GFP under control of the TH promoter.

The GFP gene was removed from pLv-MCS-GFP using BamHI and ApaI, and the sticky ends were removed by blunting with a Quick Blunting Kit (New England Biolabs, Ipswich, MA, E1202L) according to the manufacturer's specifications. The blunt ends were ligated together to create pLv-MCS-ΔGFP. The TH promoter was cloned into this construct using EcoRV and EcoRI to create pLv-MCS-THp-ΔGFP.

The Cre recombinase gene with a Myc tag was isolated from pCAG-CreMyc (purchased from Addgene, Inc., Cambridge, MA) using polymerase chain reaction (PCR) (Platinum Taq DNA Polymerase High Fidelity, Invitrogen, Carlsbad, CA, 11304-011) according to the manufacturer's specifications. Primers were purchased from IDT, Inc. (Coralville, IA). The PCR reaction added EcoRI sites to both ends of CreMyc, and a

HindIII site was added to the 3' end inside the EcoRI site. EcoRI was used to clone the CreMyc PCR product into pLv-MCS-THp-ΔGFP to create pLv-MCS-THp-CreMyc. This construct was used to generate a stable pool of HEK293 cells expressing CreMyc under control of the TH promoter.

RNA oligonucleotides for siRNA experiments and DNA oligonucleotides for shRNA experiments were synthesized by ACGT, Inc. (Wheeling, IL). DNA oligos were annealed and ligated into pENTR™/U6 using the BLOCK-iT™ U6 RNAi entry vector kit (Invitrogen, Carlsbad, CA, K4944-00) according to the manufacturer's instructions to create the plasmid shRNAs (pENTR-U6-AMPKα1&2shRNA Loops 2-4) and control shRNA (pENTR-U6-control shRNA loop 3). pENTR plasmids were transformed in One Shot TOP10 Chemically Competent E. coli cells (Invitrogen, Carlsbad, CA, C4040-10) according to the manufacturer's specifications.

An RNA polymerase III stop site flanked by two LoxP sites (LoxP-Stop-ClaI-XhoI-LoxP) was purchased as DNA oligonucleotides with 5' phosphorylated overhangs complementary to NdeI sticky ends from IDT, Inc. (Coralville, IA) and annealed. The annealed oligo contained overhangs that could be directly ligated into the pENTR-U6-AMPKα1&2shRNA-Loop3 plasmid digested with NdeI to create pENTR-U6-LoxP-AMPKα1&2shRNA-Loop3. Successful ligation of the oligo into the NdeI site of the vector removed the NdeI site, and the ligated DNA was digested with NdeI prior to transformation to remove religated vector DNA. To test the recombination, pENTR-U6-LoxP-AMPKα1&2shRNA-Loop3 DNA was recombined with Cre recombinase (New

**Table 1. Base plasmids used to create constructs**

| Plasmid name: | Use: |
|---|---|
| pLv-CMV-GFP | Base plasmid for TH promoter-driven constructs |
| 4.5ThpAL+ | Source of rat TH promoter to drive expression of GFP and CreMyc |
| pCAG-CreMyc | Source of CreMyc DNA to be cloned into TH promoter-driven construct, ubiquitously expressed CreMyc for control in transfection |
| pEGFP | Ubiquitously expressed CMV promoter-driven GFP for control in transfections |

**Table 2. Cloned constructs**

| Plasmid name: | Backbone: | Cloning strategy: | Use: | Status: |
|---|---|---|---|---|
| pLv-MCS-GFP | pLenti6 | CMV in pLv-CMV-GFP replaced with MCS | Base plasmid for TH promoter-driven GFP and CreMyc constructs | Completed |
| pLv-MCS-THp-GFP | pLenti6 | TH promoter cloned in front of GFP in pLv-MCS-GFP | Used to make TH promoter-driven GFP virus for infection and as TH promoter-driven GFP for transfection in cells | Completed |
| pLv-MCS-ΔGFP | pLenti6 | GFP gene removed from pLv-MCS-GFP | Base plasmid for TH promoter-driven CreMyc | Completed |
| pLv-MCS-THp-ΔGFP | pLenti6 | TH promoter cloned into pLv-MCS-ΔGFP | Base plasmid for TH promoter-driven CreMyc | Completed |
| pLv-MCS-THp-CreMyc | pLenti6 | CreMyc PCR product from pCAG-CreMyc cloned after TH promoter | TH promoter-driven CreMyc for transfection in cells | Completed |
| pENTR-U6-AMPKshRNA | pENTR/U6 | shRNA oligos ligated into backbone | Expression of shRNA for transfection in cells | Completed |
| pENTR-U6-LoxP-AMPK shRNA loop 3 | pENTR/U6 | LoxP oligo ligated into NdeI site in U6 promoter | Disrupted shRNA, tested with recombinant Cre | Completed |
| pENTR-U6-LoxP-AMPK shRNA loop 3-MCS | pENTR/U6 | MCS cloned after shRNA | Base plasmid for final construct | Not completed |
| pENTR-U6-LoxP-AMPK shRNA loop 3-THp-CreMyc | pENTR/U6 | THp-CreMyc from pLv-MCS-THp-CreMyc cloned after shRNA | Base plasmid for final construct | Not completed |
| pLv-BlockiT-DEST- U6-LoxP-AMPK shRNA loop 3-THp-CreMyc | pLenti6/ BLOCK-iT-DEST | U6-LoxP-AMPK shRNA-THp-CreMyc cassette from pENTR construct cloned into lentiviral backbone | Lentiviral plasmid to make final lentivirus | Not completed |

England Biolabs, Ipswich, MA, M0298S) according to the manufacturer's specifications, digested with XhoI and PvuII, and electrophoresed on a 1% agarose gel.

NIH3T3, HEK293, and PC12 cells were purchased from ATCC, Inc. (Manassas, VA), and maintained at 37$^{o}$C supplemented with 5% $CO_2$ in HyClone DMEM/High glucose (Thermo Scientific, Waltham, MA, SH30022.01) with 10% FBS (Biowest, Nuaillé, France, S01520) and 1% HyClone antibiotic/antimycotic solution (Thermo Scientific, Waltham, MA, SV30079.01). Cells were passaged at 90% confluency.

*siRNA and shRNA design*

cDNA sequences of human, mouse, and rat AMPKα1 and AMPKα2 were aligned using MacVector software. The sequence ATGATGTCAGATGGTGAATTT was identified in the NCBI database (http://www.ncbi.nlm.nih.gov/index.html) and determined to be 100% identical in all cDNAs and corresponded to the following nucleotide regions: hAMPKα1 (gene accession number Q96E92) 553-573, mAMPKα1 498-518, rAMPKα1 487-507, hAMPKα2 558-578 (gene accession number P54646.2), mAMPKα2 596-616, rAMPKα2 494-514). The global siRNA and shRNA were designed to target this region. A second sequence, AATGGAATATGTGTCTGGAGG, was 100% conserved in the cDNA sequences of human, mouse, and rat AMPKα2. This region contains two base pair mismatches with the mouse and rat AMPKα1 sequences and three base pair mismatches with the human AMPKα1 sequence. A control shRNA was designed to be identical to the AMPKα1 and 2 shRNA with the exception of 5 base pair mismatches. The sequence of the control shRNA

(ACGACGTCAGCTGGTGCATGT) did not contain significant homology to known genes in the human, mouse, or rat genomes as determined by analysis in the NCBI/BLAST program. shRNA stem loop design was based upon previous studies [TLB unpublished data, 27].

*Transfection and infection*

HEK293 cells were seeded on 60 mm plates at $1.2x10^6$ cells/plate and transfected with a 3:1 ratio of Lipofectamine2000 (Invitrogen, Carlsbad, CA, 11668019) to DNA according to the manufacturer's specifications. NIH3T3 cells were simultaneously seeded on 60 mm plates at $8x10^5$ cells/plate and transfected with a 5:1 ratio of Metafectene (Biontex, San Diego, CA, T020-1.0) to DNA according to the manufacturer's specifications. Transfection efficiency was determined by replicate transfection with ubiquitously expressed GFP (pEGFP). Cells were lysed 24, 48, or 72 hours post- siRNA transfection and 72 hours post-shRNA (pENTR-U6-AMPKα1&2 shRNA Loops 2-4) transfection for analysis. Stable pools were generated by treating transfected HEK293 cells (transfected with pLv-MCS-THp-GFP or pLv-MCS-THp-CreMyc) with 10 μg/ml Blasticidin (InvivoGen, San Diego, ant-bl-1). PC12 cells were seeded on 60 mm plates at $5x10^4$ cells/plate and infected by adding 2 ml of lentiviral THp-GFP (made from pLv-MCS-THp-GFP plasmid) for 24 hrs. Cells were maintained under standard culture conditions and examined for GFP expression after 72 hours.

*Western blotting*

Whole cell lysates were collected with Cell Lysis Buffer (Cell Signaling, Beverly, MA, 9803) supplemented with Complete Protease Inhibitor Tablets (Roche, Basel, Switzerland, #11836153001). Lysates were briefly sonicated on ice, and protein concentrations were determined by the Bradford method [41-42]. Lysates were boiled in Laemmli reducing buffer, and 50 μg of total protein from each sample was electrophoresed on 10% SDS polyacrylamide gels for AMPK isolation or 8% SDS polyacrylamide gels for ACC isolation. Proteins were transferred to an Immobilon PVDF Membrane (Millipore, Billerica, MA, IPVH08100) and blocked in Tris-buffered saline containing 0.1% Tween-20 and 5% nonfat, dry milk. Antibodies purchased from Cell Signaling (Beverly, MA, anti-AMPKα1 #2795; anti-AMPKα #2603; anti-phospho-ACC #3661; anti-ACC #3676) were used overnight at a dilution of 1:1000 in Tris-buffered saline with 0.1% Tween-20 and 5% bovine serum albumin. Antibodies purchased from GeneTex (San Antonio, TX, anti-AMPKα2,GTX111373) were used overnight at a dilution of 1:2000 in Tris-buffered saline with 0.1% Tween-20 and 5% nonfat, dry milk. Anti-actin C4 monoclonal antibody (Seven Hills Bioreagents, Cincinnati, OH) was used at a 1/10,000 dilution for 1 hr at room temperature. Anti-Myc antibody (clone 9E10) was purchased from Millipore, Inc. (Billerica, MA). Horseradish peroxidase-conjugated secondary antibodies were purchased from Promega (Madison, WI, anti-rabbit IgG, HRP conjugate #W401B; and anti-mouse IgG, HRP-conjugate #W402B) and used at a dilution of 1:25,000 for one hour. Blots were developed using SuperSignal West Pico Chemiluminescent Substrate kit (Thermo Scientific, Waltham, MA, 34080), exposed to x-ray film, and visualized by chemiluminescence.

*Data analysis*

Western blot data was analyzed with NIH ImageJ software (rsbweb.nih.gov/ij/) to quantitate protein levels. For shRNA experiments, three to six independent experiments were performed for each blot, and the results were averaged. Statistical significance was determined using one-way ANOVA.

# III. RESULTS

*siRNA-mediated knockdown of AMPK alpha*

AMPKα was first knocked down using siRNA in order to identify viable sequences that can be targeted with an shRNA to generate stable knockdown. To generate a global AMPKα1 and 2 gene knockdown, we aligned the cDNA sequences of human, mouse, and rat AMPKα1 and 2 and identified a single 21 bp sequence conserved in each (Table 3). We generated an siRNA targeting this sequence to determine if it could knock down AMPKα1 and AMPKα2 simultaneously. We also made an siRNA against a region of AMPKα2 that is conserved in human, mouse, and rat (Table 4). The siRNAs were transfected in mouse fibroblast cells, NIH3T3s, at two different concentrations, and the cells were lysed 24, 48, and 72 hours post-transfection and run on a western blot (Figure 5). The lower concentration, 20 nm, was used to ensure there were few off-target effects. The higher concentration, 100 nm, was used to ensure the greatest knockdown of the target protein. The global siRNA knocked down AMPKα1 and 2 protein levels at both concentrations at all three time points compared to mock-transfected control. The AMPKα2 siRNA caused a moderate knockdown of AMPKα1 and 2. Surprisingly, it caused a greater knockdown of AMPKα1 than AMPKα2 though the siRNA was not a perfect match for AMPKα1. The transient nature of siRNA-

**Table 3. Identification of a globally conserved sequence in AMPK alpha 1 and 2**

| | | |
|---|---|---|
| AMPKα1 | Human | AA**C** ATG ATG TCA GAT GGT GAA TTT **T**TA |
| | Mouse | AA**C** ATG ATG TCA GAT GGT GAA TTT **T**TA |
| | Rat | AA**C** ATG ATG TCA GAT GGT GAA TTT **T**TA |
| AMPKα2 | Human | AA**T** ATG ATG TCA GAT GGT GAA TTT **C**T**G** |
| | Mouse | AA**T** ATG ATG TCA GAT GGT GAA TTT **C**TA |
| | Rat | AA**T** ATG ATG TCA GAT GGT GAA TTT **C**TA |
| AMPKα1&2 global siRNA | | ATG ATG TCA GAT GGT GAA TTT |

cDNA sequences for human, mouse, and rat AMPKα1 and α2 were aligned using the MacVector software program. Mismatches are shown in bold.

**Table 4. Identification of a conserved sequence in AMPK alpha 2**

| | | |
|---|---|---|
| AMPKα1 | Human | GGT **G**AT GGA ATA TGT **C**TC **A**GG AGG **A**GA |
| | Mouse | GGT **G**AT GGA ATA TGT **C**TC TGG AGG **A**GA |
| | Rat | GGT **G**AT GGA ATA TGT **C**TC TGG AGG **A**GA |
| AMPKα2 | Human | GGT AAT GGA ATA TGT GTC TGG AGG TGA |
| | Mouse | GGT AAT GGA ATA TGT GTC TGG AGG TGA |
| | Rat | GGT AAT GGA ATA TGT GTC TGG AGG TGA |
| AMPKα2 specific siRNA | | AAT GGA ATA TGT GTC TGG AGG |

cDNA sequences for human, mouse, and rat AMPKα1 and α2 were aligned using the MacVector software program. Mismatches are shown in bold.

**Figure 5. siRNA-mediated knockdown of AMPK alpha 1 and 2 in NIH3T3 cells**

(A) Western blots of NIH3T3 cells transfected with AMPKα2 or AMPKα1&2 siRNA at 20 nM or 100 nM. Cells were lysed after 24 hrs, 48 hrs, or 72 hrs and separated with SDS-PAGE. Blots were probed with anti-AMPKα1, anti-AMPKα2, and anti-actin. Representative actin blot shown in A. (B-C) Relative AMPKα1 (B) and AMPKα2 (C) protein levels in siRNA-transfected NIH3T3 cells compared to mock-transfected control cells 24, 48, and 72 hours post-transfection after normalizing to actin loading control. Data was analyzed with NIH ImageJ software.

**Figure 5**

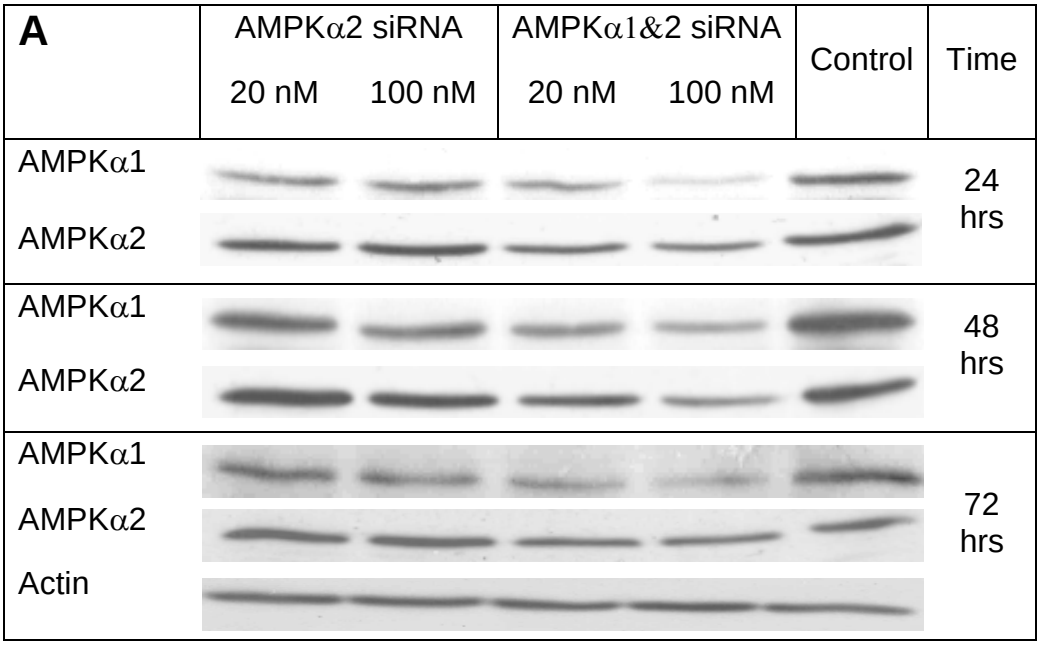
A
AMPKα2 siRNA
20 nM
100 nM
AMPKα1&2 siRNA
20 nM
100 nM
Control
Time
AMPKα1
AMPKα2
24 hrs
AMPKα1
AMPKα2
48 hrs
AMPKα1
AMPKα2
Actin
72 hrs

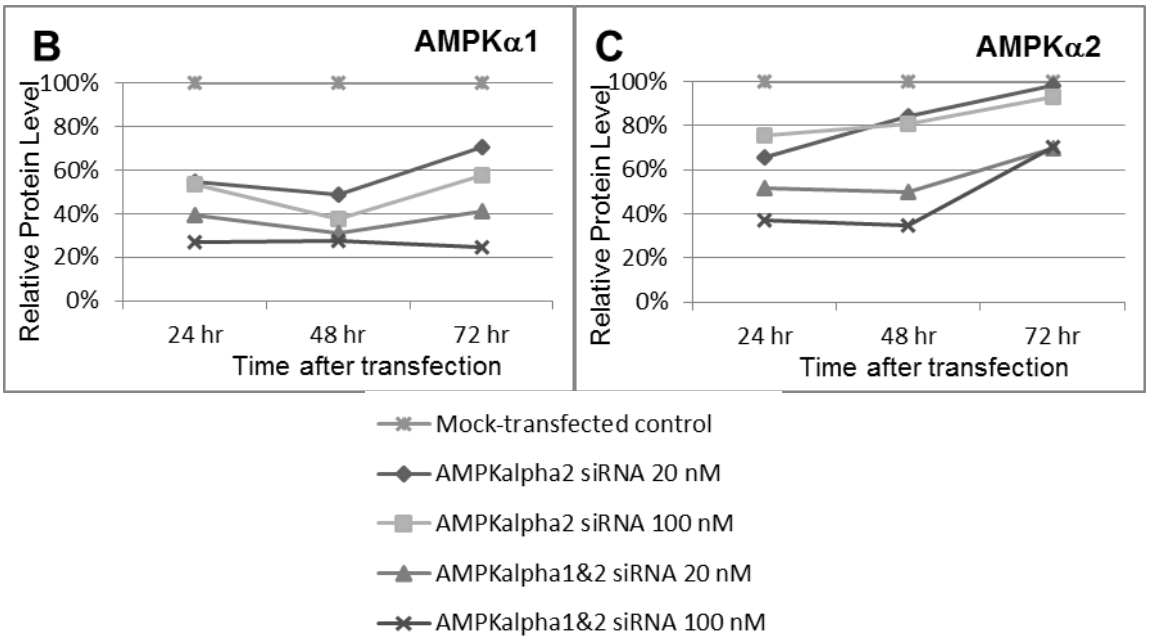
B
AMPKα1
Relative Protein Level
100%
80%
60%
40%
20%
0%
24 hr
48 hr
72 hr
Time after transfection
C
AMPKα2
Relative Protein Level
100%
80%
60%
40%
20%
0%
24 hr
48 hr
72 hr
Time after transfection
Mock-transfected control
AMPKalpha2 siRNA 20 nM
AMPKalpha2 siRNA 100 nM
AMPKalpha1&2 siRNA 20 nM
AMPKalpha1&2 siRNA 100 nM

mediated knockdown is evident in Figure 5 as a less efficient knockdown 72 hrs after transfection. These results prompted us to select the sequence of the global AMPKα1 and 2 siRNA to generate an shRNA that can be used to stably knock down AMPKα1 and 2.

*shRNA-mediated knockdown of AMPK alpha*

To generate stable knockdown of AMPKα1 and 2, we used the AMPKα1 and 2 siRNA sequence to generate an shRNA. Though the loop structure of the shRNA is cleaved prior to binding of the RNA to the target mRNA, the sequence of the loop has a significant impact on the activity of the shRNA [43]. We will refer to the most commonly used shRNA loop sequence (TTCAAGAGA) as the Brummelkamp loop [29]. However, this particular loop begins with two thymidine residues. RNA polymerase III, which drives shRNA production from the U6 promoter in the pENTR™ vector, recognizes a stretch of four or more thymidine residues as a stop site [44]. Therefore, this loop cannot be used if the stem sequence of the shRNA ends in two or more thymidine residues, as is the case for the AMPKα1 and 2 shRNA. For this reason, we needed to identify different loop sequences that did not begin with thymidine (Table 5). We tested three loops, referred to as loops 2-4, in NIH3T3 cells (Figure 6). A fourth loop, loop 1 was not tested because the plasmid was found to contain a mutation after sequencing. Two of the loops, loops 3 and 4, significantly knocked down protein levels of both isoforms of AMPKα. Loops 3 and 4 were the complement and the reverse, respectively, of the Brummelkamp loop. We found that the complement of the Brummelkamp loop,

**Table 5. Design of shRNA loop sequences and sequences of shRNA oligos**

| | |
|---|---|
| Brummelkamp loop | TTCAAGAGA |
| Loop 2 | CCACACC |
| Loop 3 | AAGTTCTCT |
| Loop 4 | AGAGAACTT |
| Loop 2 top oligo | CACCGATGATGTCAGATGGTGAATTTCC ACACCAAATTCACCATCTGACATCAT |
| Loop 2 bottom oligo | AAAAATGATGTCAGATGGTGAATTTGGT GTGGAAATTCACCATCTGACATCATC |
| Loop 3 top oligo | CACCGATGATGTCAGATGGTGAATTTAA GTTCTCTAAATTCACCATCTGACATCAT |
| Loop 3 bottom oligo | AAAAATGATGTCAGATGGTGAATTTAGA GAACTTAAATTCACCATCTGGACATCATC |
| Loop 4 top oligo | CACCGATGATGTCAGATGGTGAATTTAG AGAACTTAAATTCACCATCTGACATCAT |
| Loop 4 bottom oligo | AAAAATGATGTCAGATGGTGAATTTAAGT TCTCTAAATTCACCATCTGACATCATC |

Loop sequences and sequences of DNA oligos ordered from ACGT, Inc., and ligated into pENTR™ to create plasmid shRNAs.

**Table 6. Design of global AMPK alpha 1 and 2 shRNA and corresponding control shRNA**

| AMPKα1&2 Loop 3 shRNA sequence |
|---|
| ATG ATG TCA GAT GGT GAA TTT AAGTTCTCT<br>TAC TAC AGT CTA CCA TCC AAA |
| **Control shRNA sequence** |
| A**C**G A**C**G TCA G**C**T GGT G**C**A T**G**T AAGTTCTCT<br>T**G**C T**G**C AGT C**G**A CCA C**G**T A**C**A |

Base pair mismatches in the control shRNA are shown in bold.

**Figure 6. shRNA-mediated knockdown of AMPK alpha 1 and 2 in NIH3T3 cells with different loop sequences**

(A) Representative western blot of NIH3T3 cells transfected with AMPKα1 and 2 shRNA with loops 2-4 and control shRNA. Cells were lysed after 72 hrs. Lysates were electrophoresed with SDS-PAGE and immunoblotted with anti-AMPKα1, anti-AMPKα2, and anti-actin. (B) Relative AMPKα1 and 2 protein levels in shRNA-transfected NIH3T3 cells compared to control shRNA-transfected NIH3T3 cells after normalizing to actin loading control. Relative protein levels are listed as percentages of control. Results are representative of 3 independent experiments. Data was analyzed with NIH ImageJ software. Error bars represent the standard error of the mean. (*) $P<0.05$. (**) $P<0.01$. (***) $P<0.001$.

**Figure 6**

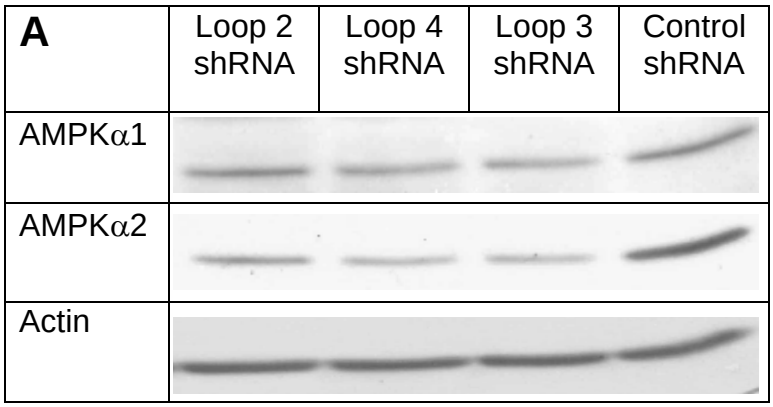
A
Loop 2 shRNA
Loop 4 shRNA
Loop 3 shRNA
Control shRNA
AMPKα1
AMPKα2
Actin

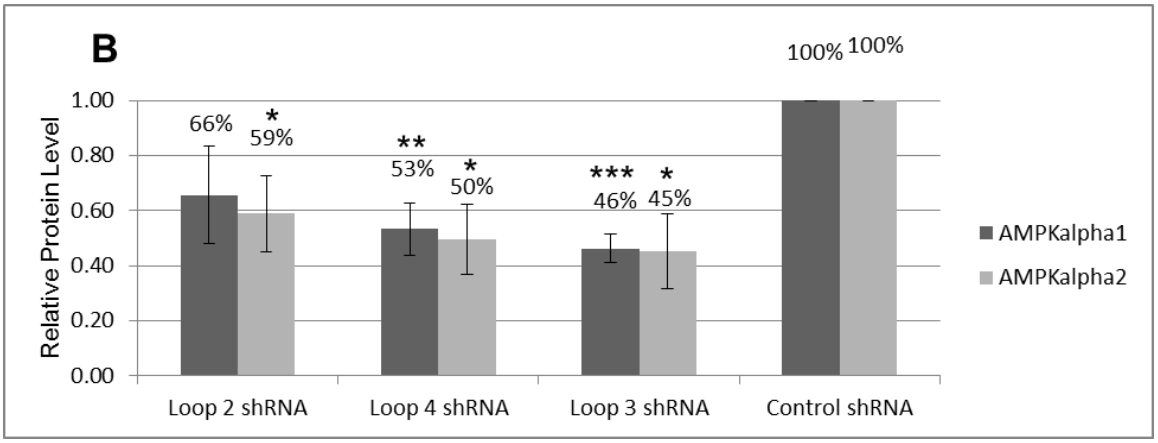
B
Relative Protein Level
1.00
0.80
0.60
0.40
0.20
0.00
66%
*
59%
**
53%
*
50%
***
46%
*
45%
100%
100%
Loop 2 shRNA
Loop 4 shRNA
Loop 3 shRNA
Control shRNA
AMPKalpha1
AMPKalpha2

loop 3, resulted in the greatest knockdown, 54% knockdown of AMPKα1 and 55% knockdown of AMPKα2, and this shRNA was chosen for further study. We created a control shRNA containing five base-pair mismatches from the target 21 nt siRNA sequence using the loop 3 sequence (Table 6). AMPKα1 and 2 protein levels in cells transfected with the control shRNA were equivalent to mock-transfected controls (data not shown). This control shRNA was used for all shRNA experiments.

*Knockdown of AMPK alpha in mouse and human cells*

We transfected the shRNA into mouse NIH3T3 cells and human embryonic kidney HEK293 cells to demonstrate its ability to knock down AMPKα1 and 2 in multiple species (Figure 7). The shRNA significantly knocked down protein levels of both isoforms of AMPKα in both species. In mouse NIH3T3 cells, AMPKα1 and AMPKα2 protein levels were knocked down 49% and 44%, respectively, compared to the control shRNA. In human HEK293 cells, AMPKα1 and AMPKα2 protein levels were knocked down 63% and 72%, respectively, compared to the control shRNA. The shRNA was likely more effective in human cells than in mouse cells due to the increased transfection efficiency in HEK293 cells, as determined by replicate transfections with GFP. Representative fluorescence micrographs of NIH3T3 and HEK293 cells transfected with GFP are shown in Figure 8 to demonstrate the difference in transfection efficiency between the cell types. Both transfections were performed as controls during shRNA experiments simultaneously and under the same conditions as the shRNA transfections. Transfection with GFP was more efficient in HEK293 cells than in NIH3T3 cells.

**Figure 7. shRNA-mediated knockdown of AMPK alpha 1 and 2 in mouse and human cells**

(A) Representative western blot of NIH3T3 and HEK293 cells transfected with AMPKα1 and 2 loop 3 shRNA and control shRNA. Cells were lysed after 72 hrs. Lysates were electrophoresed with SDS-PAGE and immunoblotted with anti-AMPKα1, anti-AMPKα2, and anti-actin. (B-C) Relative AMPKα1 and 2 protein levels in shRNA-transfected NIH3T3 cells (B) and HEK293 cells (C) compared to control shRNA-transfected cells after normalizing to actin loading control. Relative protein levels are listed as percentages of control. Results are representative of 3-6 independent experiments. Data was analyzed with NIH ImageJ software. Error bars represent the standard error of the mean. (***) $P<0.001$.

**Figure 7**

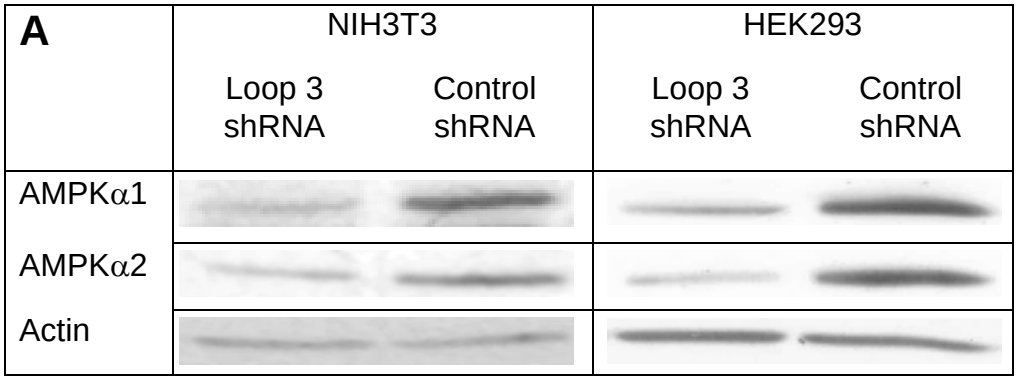
A
NIH3T3
HEK293
Loop 3 shRNA
Control shRNA
Loop 3 shRNA
Control shRNA
AMPKα1
AMPKα2
Actin

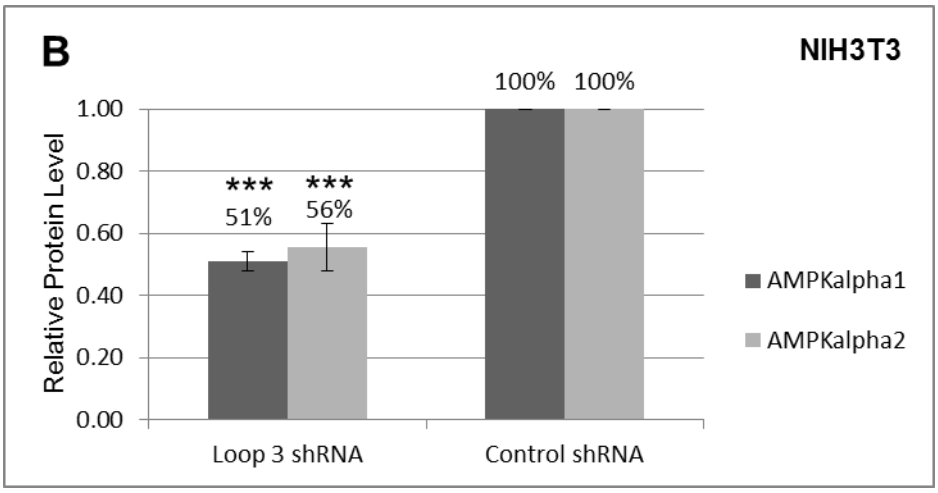
B
NIH3T3
100% 100%
1.00
0.80
0.60
0.40
0.20
0.00
Relative Protein Level
*** 51%
*** 56%
Loop 3 shRNA
Control shRNA
AMPKalpha1
AMPKalpha2

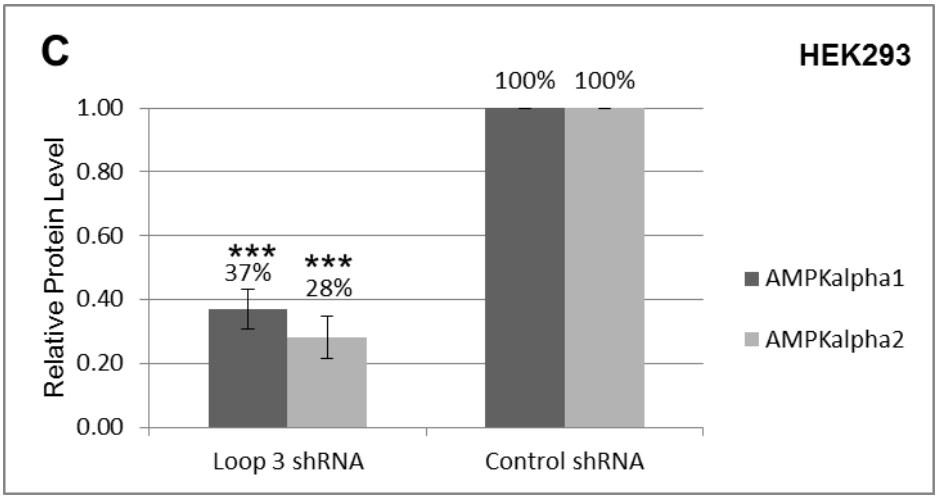
C
HEK293
100% 100%
1.00
0.80
0.60
0.40
0.20
0.00
Relative Protein Level
*** 37%
*** 28%
Loop 3 shRNA
Control shRNA
AMPKalpha1
AMPKalpha2

**Figure 8. Transfection efficiency of NIH3T3 and HEK293 cells**

(A-B) Representative fluorescence micrographs of NIH3T3 cells (A) and HEK293 cells (B) transfected with ubiquitously expressed CMV promoter-driven GFP (pEGFP) as replicate controls for shRNA transfection experiments. Fluorescence was checked after 72 hrs.

**Figure 8**

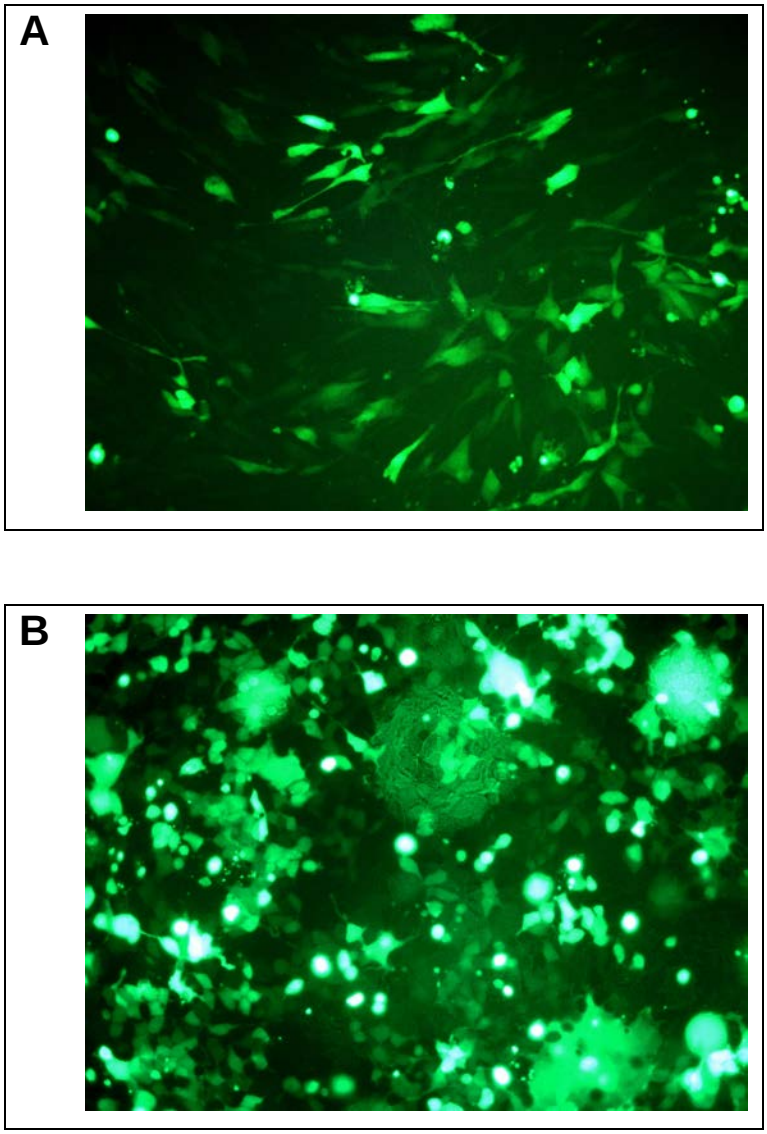

*Functional knockdown of AMPK alpha*

To show functional knockdown of AMPK by the loop 3 shRNA, we looked for reduced phosphorylation of a direct target, acetyl-CoA carboxylase (ACC). Transfection of HEK293 cells with the loop 3 AMPKα1 and 2 shRNA did not alter total ACC protein levels; however, it did cause a significant reduction in the phosphorylated form of ACC (phospho-ACC, Figure 9). The protein level of phosphorylated ACC was knocked down 41% by the AMPKα1 and 2 shRNA compared to the control shRNA. The total ACC protein levels in the AMPKα1 and 2 shRNA-treated cells compared to the control shRNA-treated cells were nearly identical and unaffected by transfection.

*Expression of TH promoter-driven constructs*

To test the expression of the tyrosine hydroxylase promoter-driven GFP plasmid (pLv-MCS-THp-GFP), we transfected HEK293 cells and selected with blasticidin to generate a stable pool of transfected cells. The cells expressed GFP (Figure 10 A), indicating the construct is functional. HEK293 cells express TH [45], even though they were isolated from kidney cells, because they have been found to more closely resemble neuronal cells than kidney cells [46]. The TH promoter-driven GFP was also expressed in PC12 cells (Figure 10 B), which are rat pheochromocytoma cells that express TH [47]. HEK293 cells were transfected with the TH-driven CreMyc plasmid (pLv-MCS-THp-CreMyc) and selected with blasticidin to generate a stable pool of cells. The extracts from these cells were run on a western blot along with positive control lysates of HEK293 cells transiently transfected with the ubiquitously expressed CreMyc plasmid (pCAG-CreMyc) (Figure 10 C). Both transfected cell populations expressed CreMy

**Figure 9. shRNA-mediated knockdown of AMPK alpha activity in HEK293 cells**

(A) Representative western blot of HEK293 cells transfected with AMPK$\alpha$1 and 2 loop 3 shRNA and control shRNA. Cells were lysed after 72 hrs. Lysates were electrophoresed on an 8% SDS-PAGE gel and immunoblotted with anti-phospho-ACC, anti-ACC, and anti-actin. Lysates from one experiment were also electrophoresed on a 10% SDS-PAGE gel and immunoblotted with anti-AMPK$\alpha$ and anti-actin. (B) Phospho-ACC protein levels in shRNA-transfected HEK293 cells compared to control shRNA-transfected cells as a percentage of total ACC levels after normalizing to actin loading control. Relative protein levels are listed as percentages of control. Results are representative of 3 independent experiments. Data was analyzed with NIH ImageJ software. Error bars represent the standard error of the mean. (**) $P<0.01$.

**Figure 9**

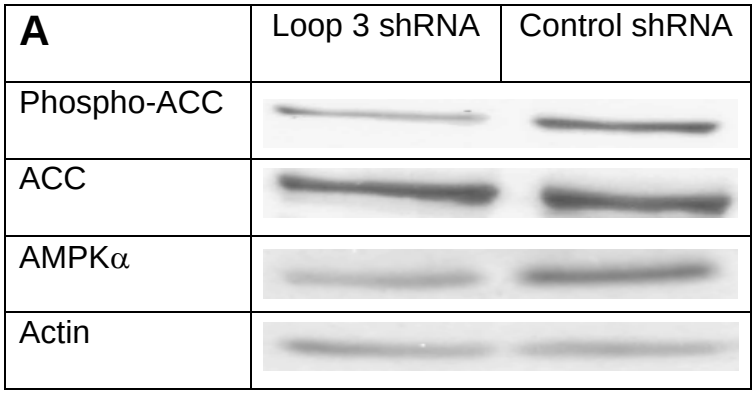
A
Loop 3 shRNA
Control shRNA
Phospho-ACC
ACC
AMPKα
Actin

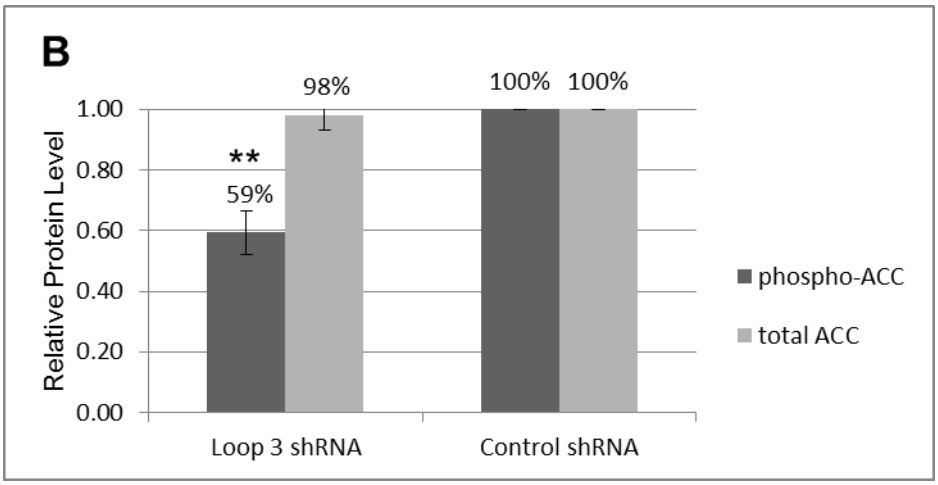
B
Relative Protein Level
1.00
0.80
0.60
0.40
0.20
0.00
**
59%
98%
100%
100%
Loop 3 shRNA
Control shRNA
phospho-ACC
total ACC

**Figure 10. Expression of TH promoter-driven constructs**

(A) Fluorescence micrograph of HEK293 cells transfected with TH promoter-driven GFP plasmid (pLv-MCS-THp-GFP). Transiently transfected cells were selected with 10 μg/ml Blasticidin to generate a stable pool of transfected cells. (B) Fluorescence micrograph of PC12 cells infected with TH promoter-driven GFP lentivirus. (C) Western blot of HEK293 cells transfected with TH promoter-driven CreMyc plasmid (pLv-MCS-THp-CreMyc) and ubiquitously expressed CreMyc plasmid (pCAG-CreMyc). Cells were lysed after 72 hrs. Lysates were electrophoresed on a 10% SDS-PAGE gel and immunoblotted with anti-Myc.

**Figure 10**

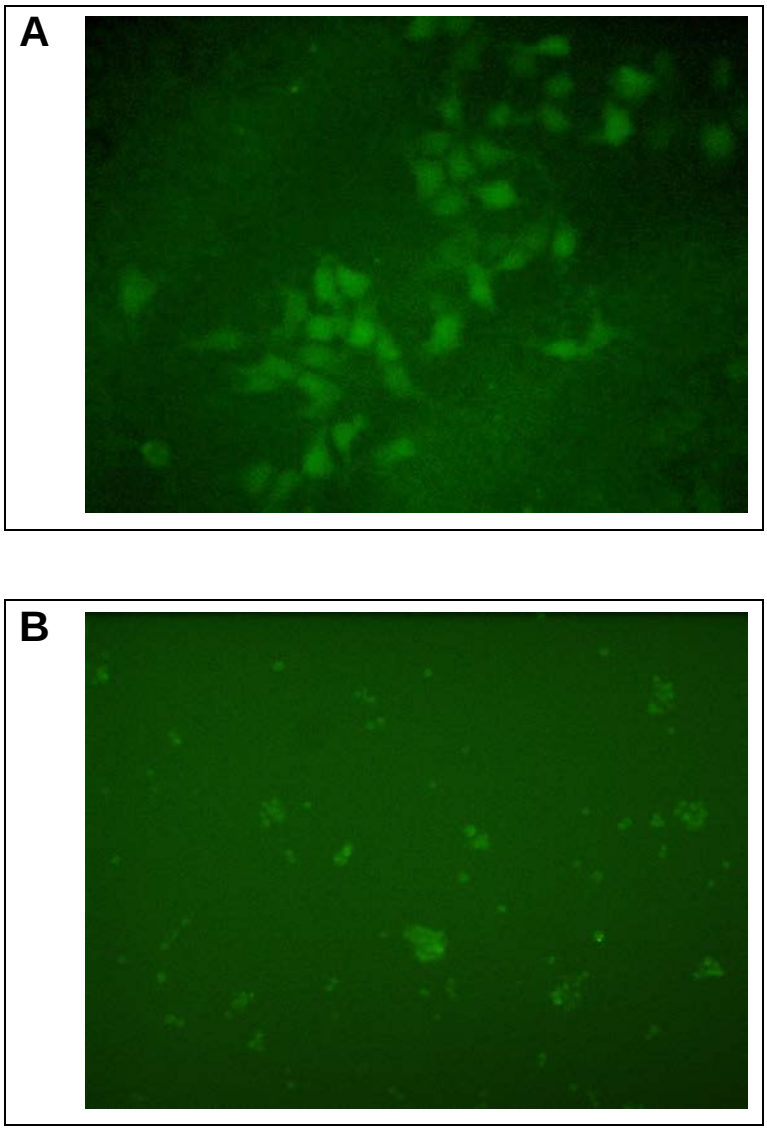


| C | Untransfected | TH-Cre-Myc | pCAG-Cre-Myc |
|---|---|---|---|
| Myc | | | |

(38 kDa), and all HEK293 cell populations did not express endogenous Myc (49 kDa) as expected [48].

*Cre recombinase-driven recombination*

The U6 promoter was disrupted with two LoxP sites flanking an RNA polymerase III stop site. The DNA was tested with recombinant Cre to ensure the floxed sequence was removed. The recombined DNA was digested with XhoI and PvuII and electrophoresed on an agarose gel to determine the size of the resulting fragments (Figure 11). The recombination removed 52 bp, including the XhoI site, from the DNA. This can be seen in the gel as a decrease in the amount of 770 and 279 bp fragments and the appearance of a 997 bp fragment (indicated with an arrow). The reaction is reversible, so the reaction proceeds to equilibrium. The banding pattern indicates the recombination occurred as expected.

**Figure 11. *In vitro* recombination of disrupted U6 promoter construct with Cre recombinase**

Agarose gel of pENTR-U6-LoxP-AMPKα1&2shRNA Loop 3 construct recombined with Cre recombinase. Lane 1 contains a ladder. Lanes 2 and 3 contain pENTR-U6-LoxP-AMPKα1&2shRNA DNA digested with XhoI and PvuII. Lane 3 was recombined with Cre recombinase prior to digestion.

**Figure 11**

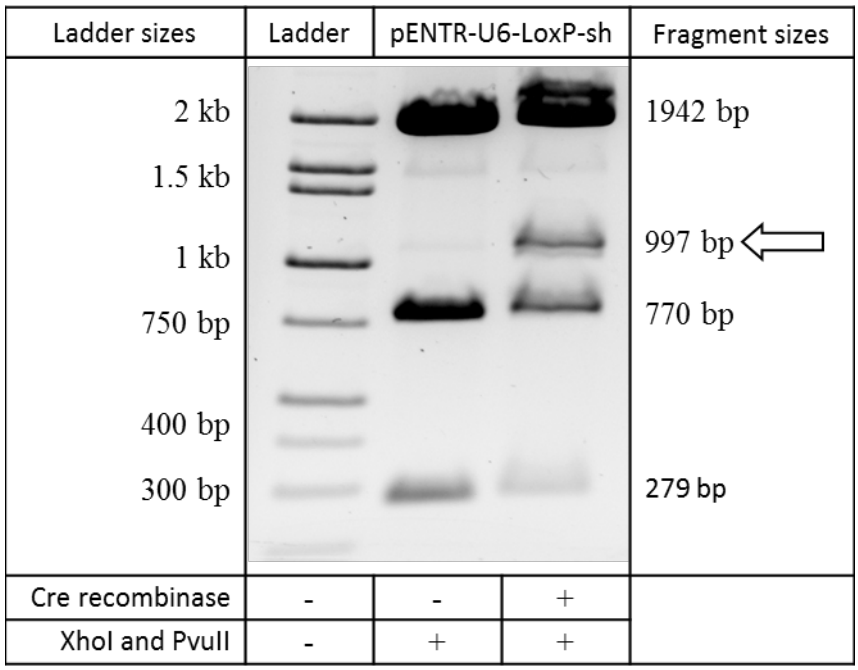
Ladder sizes
Ladder
pENTR-U6-LoxP-sh
Fragment sizes
2 kb
1.5 kb
1 kb
750 bp
400 bp
300 bp
1942 bp
997 bp
770 bp
279 bp
Cre recombinase
-
-
+
XhoI and PvuII
-
+
+

# IV. DISCUSSION

*AMPK alpha 1 and 2 knockdown*

AMPK is a key regulator of cellular metabolism, and it exerts its function through the catalytic alpha subunit. Knocking down both isoforms of the catalytic subunit is a way to study the function of AMPK; however, previous knockdowns of AMPKα were only designed to be effective in one model system. We originally tested an shRNA against AMPKα1 and 2 that had been previously published [34], but the target sequence was not conserved between multiple species. Therefore, we were unable to test the knockdown in a convenient system. This led us to develop an siRNA that can target both catalytic α1 and α2 isoforms of AMPK in human, mouse, and rat cells. This new siRNA could be used in any number of systems because the sequence is conserved. Because siRNA only causes a transient knockdown in protein levels, we converted the siRNA into an shRNA. The shRNA caused a significant reduction in AMPKα protein levels in both human and mouse cells. We hypothesize the shRNA will also be effective in rat cells because the sequence is 100% conserved.

When designing an shRNA, the loop that is used can have a significant impact on the knockdown of the target protein [43]. We chose to test three different loops to

determine which is the most effective. The complement of the most commonly reported loop (loop 3) was found to be the most effective. This loop can be used for shRNAs that end in thymidine residues as an alternative to the most common loop to prevent the formation of an RNA polymerase III stop site.

The shRNA was cloned into the pENTR™/U6 Entry vector from Invitrogen. From this plasmid, the shRNA can be transferred into other expression systems such as the lentiviral Block-iT™ Dest vector from Invitrogen, which can be used to make a lentivirus containing the shRNA. Lentiviral infection with the shRNA should cause greater knockdown due to a higher efficiency of transduction.

Knockdown of protein levels does not necessarily correspond to a reduction in activity of the target protein. For this reason, we wanted to ensure AMPKα activity was also reduced by the shRNA. ACC is phosphorylated at Ser79 by AMPKα [49]. ACC catalyzes the production of malonyl-CoA from acetyl-CoA, thus providing the starting material for fatty acid synthesis. When ATP is depleted from the cell, ACC is inactivated by AMPK, and acetyl-CoA is used for energy production in the citric acid cycle. The reduction in phospho-ACC levels indicates that AMPK activity, not just protein levels, was reduced by the shRNA.

*Tissue-specific constructs*

The tyrosine hydroxylase promoter will be used to generate tissue-specific expression of the shRNA. A plasmid containing TH promoter-driven GFP was generated

to visualize where the TH promoter was expressed. GFP was expressed in HEK293 and PC12 cells, which are TH positive, so the promoter is functional. Also, the PC12 cells were infected with a lentivirus containing TH promoter-driven GFP. This lentivirus was over 12 kb in size. The generally accepted size limit for a lentivirus to be efficiently packaged into viral particles is about 10 kb. The expression of GFP in these cells indicates that a larger virus is still capable of being effectively packaged and infecting cells. This is important because the final virus will be about 12 kb, so we would expect the final virus to be functional from this result.

A plasmid containing TH promoter-driven Cre recombinase with a Myc tag (pLv-MCS-THp-CreMyc) was generated to direct tissue-specific expression of Cre recombinase. Cre, when used with the shRNA with a disrupted promoter, will restore the promoter and allow the shRNA to be made in TH positive cells only. The Myc tag was detected in lysates of a stable pool of HEK293 cells transfected with pLv-MCS-THp-CreMyc, indicating the plasmid is functional.

*Disrupted U6 promoter*

The U6 promoter of the shRNA was disrupted by a floxed sequence of DNA containing an RNA polymerase III stop site. The cloning to create this construct was challenging because the floxed sequence of DNA was ordered as small, approximately 90 bp, DNA oligos that were annealed and digested before ligation into the NdeI site of the vector. The small size of the insert and the lack of directional cloning made the reaction very unfavorable. To overcome this issue, we designed oligos that would have overhangs

following annealing that are complementary to the NdeI site in the vector. The oligos were synthesized with phosphorylated 5' ends, which are required by DNA ligase, to allow them to be ligated directly into the digested vector following annealing. Ligation of this oligo into the vector would remove the NdeI site in the vector, so we were able to digest the ligated DNA with NdeI before transformation to get rid of any vector DNA that religated with itself. This strategy selected for successful ligations and removed the large amount of background vector religation. The floxed sequence of DNA was removed from the promoter *in vitro* following treatment with Cre recombinase. This indicates the floxed sequence is able to be removed as expected, and the promoter should be restored following expression of Cre recombinase.

*Future work*

In the future, the HEK293 cells stably expressing TH promoter-driven CreMyc will be transfected with the shRNA with a disrupted promoter to test the recombination mediated by Cre to determine if the U6 promoter function is restored following excision of the floxed sequence. The TH-driven plasmids must also be tested to ensure they are truly tissue specific and are not expressed in TH negative cells. In order to make the final virus, the cassette containing the TH promoter-driven Cre recombinase will be transferred to the same vector as the shRNA with the disrupted promoter.

The construct with the disrupted promoter must still be tested to determine if the shRNA is no longer expressed. If the floxed sequence of DNA is not sufficient to disrupt the U6 promoter, and there is still some expression of the shRNA, a GFP reporter gene

can be cloned into the sequence. This reporter gene is very large and will effectively prevent transcription from the promoter. The construct with the disrupted promoter must also be tested to determine if the shRNA is expressed after recombination with Cre recombinase. Following recombination with Cre, one 34 basepair LoxP site remains in the DNA. The distance between crucial elements of the U6 promoter is critical to its proper function, but the sequence of DNA between the elements is not [50]. If the extra DNA from the LoxP site prevents efficient binding of RNA polymerase III to the restored U6 promoter, an alternate strategy is to remove part of the U6 promoter so the LoxP site remaining after recombination replaces it. This should ensure the promoter will be functional following recombination.

In future studies, the tissue-specific shRNA will be used to generate a rat transgenic strain with knockdown of AMPKα1 and 2 only in cells that express TH. A lentivirus containing both the shRNA with the disrupted U6 promoter and the TH promoter-driven Cre recombinase will be used to infect fertilized rat embryos. A technique called embryo transfer will be used to transplant the infected embryos into pseudopregnant mothers [51-52]. The pups will have the transgene integrated into every cell, but the shRNA will only be made in cells that express TH. Therefore, the rats will have tissue-specific knockdown of AMPKα1 and 2. We expect the knockdown should not result in embryonic lethality because it is not a complete knockout, so some AMPKα protein is still made, and it is only knocked down in some tissues. Previously, a mouse strain with total body knockout of AMPKα1 and liver-specific knockout of AMPKα2 was generated [3,18]. The mice were viable, so this indicates that tissue-specific double

knockout models are possible, although it is currently not known which tissues require expression of AMPKα1 and 2 for survival of the animals. It is also important to remember that the rats will have knockdown of AMPKα1 and 2, not knockout. It is possible that minimal expression of AMPKα1 and 2 could allow the animals to survive. If the animals are not viable, an alternative is to use a conditional expression system, such as a Tet-On system [53], to control the temporal expression of Cre recombinase. Using this system, Cre recombinase would not be expressed in TH-positive tissues until the animals are treated with the antibiotic tetracycline or a derivative, doxycycline. In this way, knockdown of AMPK would not occur until after the animals are already born, so defects in development would be avoided. The rats will be used in future studies to determine if breathing regulation by carotid body type I cells is impaired by knockdown of AMPK. If AMPK is necessary for carotid body type I cells to respond to hypoxia, the rats will not be able to upregulate their breathing rate in response to hypoxia. These studies will help elucidate the role of AMPK in oxygen sensing by the carotid body.

In conclusion, we have generated a new shRNA that can significantly knock down protein levels and activity of AMPKα1 and 2 in multiple species. This shRNA will later be used to generate a transgenic rat strain with tissue-specific knockdown of AMPKα1 and 2.

# V. APPENDIX

## Abbreviations

AMPK- 5'-Adenosine Monophosphate-Activated Protein Kinase

PRKAA- Protein-Kinase, AMP-activated

ACC- Acetyl-CoA Carboxylase

CaMKKβ- Calmodulin-Dependent Protein Kinase Kinase β

AICAR- 5-Aminoimidazole-4-Carboxyamide Ribonucleoside

RNAi- RNA Interference

dsRNA- Double-Stranded RNA

siRNA- Small Interfering RNA

RISC- RNA-Induced Silencing Complex

shRNA- Short Hairpin RNA

miRNA- Micro RNA

TH- Tyrosine Hydroxylase

MCS- Multiple Cloning Site

GFP- Green Fluorescent Protein

PCR- Polymerase Chain Reaction

# VI. REFERENCES

[1] S. Dale, W.A. Wilson, A.M. Edelman, D.G. Hardie, Similar substrate recognition motifs for mammalian AMP-activated protein kinase, higher plant HMG-CoA reductase kinase-A, yeast SNF1, and mammalian calmodulin-dependent protein kinase I, FEBS Lett. 361 (1995) 191-195.

[2] J. Zhou, W. Huang, R. Tao, S. Ibaragi, F. Lan, Y. Ido, X. Wu, Y.O. Alekseyev, M.E. Lenburg, G.F. Hu, Z. Luo, Inactivation of AMPK alters gene expression and promotes growth of prostate cancer cells, Oncogene 28 (2009) 1993-2002.

[3] B. Viollet, Y. Athea, R. Mounier, B. Guigas, E. Zarrinpashneh, S. Horman, L. Lantier, S. Hebrard, J. Devin-Leclerc, C. Beauloye, M. Foretz, F. Andreelli, R. Ventura-Clapier, L. Bertrand, AMPK: Lessons from transgenic and knockout animals, Front. Biosci. 14 (2009) 19-44.

[4] S. Horman, G. Browne, U. Krause, J. Patel, D. Vertommen, L. Bertrand, A. Lavoinne, L. Hue, C. Proud, M. Rider, Activation of AMP-activated protein kinase leads to the phosphorylation of elongation factor 2 and an inhibition of protein synthesis, Curr. Biol. 12 (2002) 1419-1423.

[5] DG. Hardie, AMP-activated protein kinase: a cellular energy sensor with a key role in metabolic disorders and in cancer, Biochem. Soc. Trans. 2011 39 (2011) 1-13.

[6] G.R. Steinberg, B.E. Kemp, AMPK in Health and Disease, Physiol. Rev. 89 (2009) 1025-1078.

[7] D. Carling, AMP-activated protein kinase: balancing the scales, Biochimie 87 (2005) 87-91.

[8] D.G. Hardie, AMP-activated/SNF1 protein kinases: conserved guardians of cellular energy, Nat. Rev. Mol. Cell Biol. 8 (2007) 774-785.

[9] B. Viollet, F. Andreelli, S.B. Jørgensen, C. Perrin, D. Flamez, J. Mu, J.F. Wojtaszewski, F.C. Schuit, M. Birnbaum, E. Richter, R. Burcelin, S. Vaulont, Physiological role of AMP-activated protein kinase (AMPK): insights from knockout mouse models, Biochem. Soc. Trans. 31 (2003) 216-219.

[10] K.M. Neurath, M.P. Keough, T. Mikkelsen, K.P. Claffey, AMP-dependent protein kinase alpha 2 isoform promotes hypoxia-induced VEGF expression in human glioblastoma, Glia 53 (2006) 733-743.

[11] S.A. Hawley, F.A. Ross, C. Chevtzoff, K.A. Green, A. Evans, S. Fogarty, M.C. Towler, L.J. Brown, O.A. Ogunbayo, A.M. Evans, D.G. Hardie, Use of cells expressing gamma subunit variants to identify diverse mechanisms of AMPK activation, Cell Metab. 11 (2010) 554-565.

[12] S.H. Park, S.R. Gammon, J.D. Knippers, S.R. Paulsen, D.S. Rubink, W.W. Winder, Phosphorylation-activity relationships of AMPK and acetyl-CoA carboxylase in muscle, J. Appl. Physiol. 92 (2002) 2475-2482.

[13] Emerling BM, Weinberg F, Snyder C, Burgess Z, Mutlu GM, Viollet B, Budinger GR, Chandel NS, Hypoxic activation of AMPK is dependent on mitochondrial ROS but independent of an increase in AMP/ATP ratio, Free Radic. Biol. Med. 46 (2009) 1386-1391.

[14] M. Suter, U. Riek, R. Tuerk, U. Schlattner, T. Wallimann, D. Neumann, Dissecting the role of 5'-AMP for allosteric stimulation, activation, and deactivation of AMP-activated protein kinase, J. Biol. Chem. 281 (2006) 32207-32216.

[15] C. Peers, C.N. Wyatt, A.M. Evans, Mechanisms for acute oxygen sensing in the carotid body, Respir. Physiol. Neurobiol. 174 (2010) 292-298.

[16] C. Gonzalez, L. Almaraz, A. Obeso, R. Rigual, Carotid body chemoreceptors: from natural stimuli to sensory discharges, Physiol. Rev. 74 (1994) 829-898.

[17] A.M. Evans, K.J. Mustard, C.N. Wyatt, C. Peers, M. Dipp, P. Kumar, N.P. Kinnear, D.G. Hardie, Does AMP-activated protein kinase couple inhibition of mitochondrial oxidative phosphorylation by hypoxia to calcium signaling in O2-sensing cells?, J. Biol. Chem. 280 (2005) 41504-41511.

[18] B. Guigas, N. Taleux, M. Foretz, D. Detaille, F. Andreelli, B. Viollet, L. Hue, AMP-activated protein kinase-independent inhibition of hepatic mitochondrial oxidative phosphorylation by AICA riboside, Biochem. J. 404 (2007) 499-507.

[19] J. Bain, L. Plater, M. Elliott, N. Shpiro, CJ. Hastie, H. McLauchlan, I. Klevernic, JS. Arthur, DR. Alessi, P. Cohen, The selectivity of protein kinase inhibitors: a further update, Biochem. J. 408 (2007) 297-315.

[20] S.B. Jørgensen, J.F. Wojtaszewski, B. Viollet, F. Andreelli, J.B. Birk, Y. Hellsten, P. Schjerling, S. Vaulont, P.D. Neufer, E.A. Richter, H. Pilegaard, Effects of alpha-AMPK knockout on exercise-induced gene activation in mouse skeletal muscle, FASEB J. 19 (2005) 1146-1148.

[21] A. Fire, S. Xu, M.K. Montgomery, S.A. Kostas, S.E. Driver, C.C. Mello, Potent and specific genetic interference by double-stranded RNA in Caenorhabditis elegans, Nature 391 (1998) 806-811.

[22] S.M. Hammond, E. Bernstein, D. Beach, G.J. Hannon, An RNA-directed nuclease mediates post-transcriptional gene silencing in Drosophila cells, Nature 404 (2000) 293-296.

[23] S.M. Hammond, S. Boettcher, A.A. Caudy, R. Kobayashi, G.J. Hannon, Argonaute2, a link between genetic and biochemical analysis of RNAi, Science 293 (2001) 1146-1150.

[24] M. Scherr, M.A. Morgan, M. Eder, Gene silencing mediated by small interfering RNAs in mammalian cells, Curr. Med. Chem. 10 (2003) 245-256.

[25] N. Doi, S. Zenno, R. Ueda, H. Ohki-Hamazaki, K. Ui-Tei, K. Saigo, Short-interfering-RNA-mediated gene silencing in mammalian cells requires Dicer and eIF2C translation initiation factors, Curr. Biol. 13 (2003) 41-46.

[26] D.D. Rao, J.S. Vorhies, N. Senzer, J. Nemunaitis, siRNA vs. shRNA: similarities and differences, Adv. Drug Deliv. Rev. 61 (2009) 746-759.

[27] E. Bernstein, A.A. Caudy, S.M. Hammond, G.J. Hannon, Role for a bidentate ribonuclease in the initiation step of RNA interference, Nature 409 (2001) 363-366.

[28] T.R. Brummelkamp, R. Bernards, R. Agami, Stable suppression of tumorigenicity by virus-mediated RNA interference, Cancer Cell 2 (2002) 243-247.

[29] T.R. Brummelkamp, R. Bernards, R. Agami, A system for stable expression of short interfering RNAs in mammalian cells, Science 296 (2002) 550-553.

[30] J. Harborth, S.M. Elbashir, K. Vandenburgh, H. Manninga, S.A. Scaringe, K. Weber, T. Tuschl, Sequence, chemical, and structural variation of small interfering RNAs and short hairpin RNAs and the effect on mammalian gene silencing, Antisense Nucleic Acid Drug Dev. 13 (2003) 83-105.

[31] S.M. Elbashir, J. Harbouth, W. Lendeckel, A. Yalcin, K. Weber, T. Tuschl, Duplexes of 21-nucleotide RNAs mediate RNA interference in cultured mammalian cells, Nature 411 (2001) 494-498.

[32] P.J. Paddison, A.A. Caudy, E. Bernstein, G.J. Hannon, D.S. Conklin, Short hairpin RNAs (shRNAs) induce sequence-specific silencing in mammalian cells, Genes Dev. 16 (2002) 948-958.

[33] L. Vucicevic, M. Misirkic, K. Janjetovic, L. Harhaji-Trajkovic, M. Prica, D.

Stevanovic, E. Isenovic, E. Sudar, M. Sumarac-Dumanovic, D. Micic, V. Trajkovic, AMP-activated protein kinase-dependent and –independent mechanisms underlying in vitro antiglioma action of compound C, Biochem. Pharmacol. 77 (2009) 1684-1693.

[34] V. Aguilar, S. Alliouachene, A. Sotiropoulos, A. Sobering, Y. Athea, F. Djouadi, S. Miraux, E. Thiaudiére, M. Foretz, B. Viollet, P. Diolez, J. Bastin, P. Benit, P. Rustin, D. Carling, M. Sandri, R. Ventura-Clapier, M. Pende, S6 kinase depletion suppresses muscle growth adaptations to nutrient availability by activating AMP kinase, Cell Metab. 5 (2007) 476-487.

[35] D.L. Hamilton, K. Abremski, Site-specific recombination by the bacteriophage P1 lox-Cre system: Cre-mediated synapsis of two lox sites, J. Mol. Biol. 178 (1984) 481-486.

[36] M. Lewandoski, K.M. Wassarman, G.R. Martin, Zp3-cre, a transgenic mouse line for the activation or inactivation of loxP-flanked target genes specifically in the female germ line, Curr. Biol. 7 (1997) 148-151.

[37] H. Gu, J.D. Marth, P.C. Orban, H. Mossmann, K. Rajewsky, Deletion of a DNA polymerase beta gene segment in T cells using cell type-specific gene targeting, Science 265 (1994) 103-106.

[38] P.B. Molinoff, J. Axelrod, Biochemistry of catecholamines, Ann. Rev. Biochem. 40 (1971) 465-500.

[39] P. Ortega-Sáenz, A. Pascual, R. Gómez-Díaz, J. López-Barneo, Acute oxygen sensing in heme oxygenase-2 null mice, J. Gen. Physiol. 128 (2006) 405-411.

[40] J. Lindeberg, D. Usoskin, H. Bengtsson, A. Gustafsson, A. Kylberg, S. Söderström, T. Ebendal, Transgenic expression of cre recombinase from the tyrosine hydroxylase locus, Genesis 40 (2004) 67-73.

[41] A.D. Gultice, K. Kulkarni-Datar, T.L. Brown, Hypoxia-inducible factor 1alpha (HIF1A) mediates distinct steps of rat trophoblast differentiation in gradient oxygen, Biol. Reprod. 80 (2009) 184-193.

[42] M.M. Bradford, A rapid and sensitive method for the quantitation of microgram quantities of protein utilizing the principle of protein-dye binding, Anal. Biochem. 72 (1976) 248-254.

[43] N.C. Schopman, Y.P. Liu, P. Konstantinova, O. ter Brake, B. Berkhout, Optimization of shRNA inhibitors by variation of the terminal loop sequence, Antiviral Res. 86 (2010) 204-211.

[44] E.P. Geiduscheck, G.P. Tocchini-Valentini, Transcription by RNA polymerase III, Ann. Rev. Biochem. 57 (1988) 873-914.

[45] M. Orth, S.J. Tabrizi, C. Tomlinson, K. Messmer, L.V. Korlipara, A.H. Schapira, J.M. Cooper, G209A mutant alpha synuclein expression specifically enhances dopamine induced oxidative damage, Neurochem. Int. 45 (2004) 669-676.

[46] G. Shaw, S. Morse, M. Ararat, F.L. Graham, Preferential transformation of human neuronal cells by human adenoviruses and the origin of HEK 293 cells, FASEB J. 16 (2002) 869-871.

[47] W.R. Paulding, P.O. Schnell, A.L. Bauer, J.B. Striet, J.A. Nash, A.V. Kuznetsova, M.F. Czyzyk-Krzeska, Regulation of gene expression for neurotransmitters during adaptation to hypoxia in oxygen-sensitive neuroendocrine cells, Microsc. Res. Tech. 59 (2002) 178-187.

[48] C. Wellerdieck, M. Oles, L. Pott, S. Korsching, G. Gisselmann, H. Hatt, Functional expression of odorant receptors of the zebrafish *Danio rerio* and of the nematode *C. elegans* in HEK293 cells, Chem. Senses 22 (1997) 467-476.

[49] J. Ha, S. Daniel, S.S. Broyles, K.H. Kim, Critical phosphorylation sites for acetyl-CoA carboxylase activity, J. Biol. Chem. 269 (1994) 22162-22168.

[50] M.R. Paule, R.J. White, Transcription by RNA polymerases I and III, Nucleic Acids Res. 28 (2000) 1283-1298.

[51] C. Sjöblom, C.T. Roberts, M. Wikland, S.A. Robertson, Granulocyte-macrophage colony-stimulating factor alleviates adverse consequences of embryo culture on fetal growth trajectory and placental morphogenesis, Endocrinology 146 (2005) 2142-2153.

[52] C. Lois, E.J. Hong, S. Pease, E.J. Brown, D. Baltimore, Germline transmission and tissue-specific expression of transgenes delivered by lentiviral vectors, Science 295 (2002) 868-872.

[53] M. Gossen, J. Bujard, Tight control of gene expression in mammalian cells by tetracycline-responsive promoters, Proc. Natl. Acad. Sci. USA 89 (1992) 5547-5551.